To the Graduate Council:

I am submitting herewith a thesis written by R. David Turner entitled "Self-Correcting, Non-Externally Controlled Computer-Guided Vehicle." I have examined the final copy of this thesis for form and content and recommend that it be accepted in partial fulfillment of the requirements for the degree of Master of Science, with a major in Mechanical Engineering.

Frank H. Speckhart, Major Professor

We have read this thesis
and recommend its acceptance:

Clement C. Wilson

James A. Euler

Accepted for the Council:

C W Minkel

Vice Provost
and Dean of the Graduate School

STATEMENT OF PERMISSION TO USE

In presenting this thesis in partial fulfillment of the requirements for a Master's degree at the University of Tennessee, Knoxville, I agree that the Library shall make it available to borrowers under the rules of the Library. Brief quotations from this thesis are allowable without special permission, provided that accurate acknowledgement of the source is made.

Permission for extensive quotation from or reproduction of this thesis may be granted by my major professor, or in his absence, by the Head of Interlibrary Services when, in the opinion of either, the proposed use of the material is for scholarly purposes. Any copying or use of the material in this thesis for financial gain shall not be allowed without my written permission.

Signature David Turner

Date May 24, 1991

SELF-CORRECTING, NON-EXTERNALLY CONTROLLED COMPUTER-GUIDED VEHICLE

A Thesis

Presented for the

Master of Science

Degree

The University of Tennessee, Knoxville

R. David Turner

August 1991

ACKNOWLEDGEMENTS

I wish to thank Dr. Frank Speckhart, my major professor, for his help and guidance during my work on this project.

I am grateful to Dr. James Euler, for his patience and timely solutions.

I also wish to thank Dr. Clement Wilson, for his interest and support.

I appreciate all of the help and insight bestowed upon me by Mr. Daniel Graham and Mr. Gary Hatmaker, machinists for the CGV prototype.

I am indebted to Mr. Dennis Higdon, senior electronics technician, for his extreme patience and interest.

I would also like to recognize the support received from my fellow graduate students throughout the course of this study.

ABSTRACT

Many Automated Guided Vehicles currently in use are dependent upon external means for their source of guidance. These external guidance devices range from electric wires to cables placed on the floor. To get away from external control of the vehicles it was conceptualized to control a vehicle of this nature strictly by internal means. The complete control of this vehicle would be commanded by a portable laptop computer. The basic concept would be to enter in the desired path the programmer wants the vehicle to follow, then by relying on sensors to give the velocity of the vehicle the position is determined by an integration scheme.

The main purpose of this thesis is to study the feasibility of this particular guidance vehicle. In this thesis is a discussion of the prototypes design, performance results, and recommendations.

TABLE OF CONTENTS

CHAPTER PAGE

1. INTRODUCTION....1
   1.1 BACKGROUND....1
   1.2 OBJECTIVES....2
   1.3 SCOPE....2

2. PROTOTYPE OVERVIEW....4
   2.1 CGV OPERATION OVERVIEW....4
   2.2 PROTOTYPE EQUIPMENT AND OPERATION....8
   2.3 PROTOTYPE CIRCUITRY AND OPERATION....15
   2.4 PROTOTYPE STRUCTURE AND OPERATION....20
   2.5 CGV OPERATION OVERVIEW....26

3. CGV CORRECTION ANGLE CONTROL SCHEME....30
   3.1 CONTROL SCHEME OVERVIEW....30
   3.2 CONTROL SCHEME DEVELOPMENT....32
   3.3 CGV STABILITY....39

4. PERFORMANCE TESTING OF THE PROTOTYPE....40
   4.1 STRAIGHT LINE PATH TEST....40
   4.2 TEST SETUP....41
   4.3 DISCUSSION OF RESULTS....43
   4.4 CGV STABILITY....50

5. DISCUSSION OF PROTOTYPE ERROR....56
   5.1 ENCODER ERROR TESTS....56
   5.2 ACTUAL TEST RUNS....56
   5.3 RUNNING AVERAGE....61
   5.4 CONSTANT STEERING ANGLE....64
   5.5 RADIUS OF CURVATURE TESTS....67
   5.6 BELT SLIP TEST....69

6. DISCUSSION OF CONTROL SCHEME PERFORMANCE....70

7. RECOMMENDATIONS....72

BIBLIOGRAPHY....74

APPENDICES....76

   APPENDIX A. PROGRAM LISTING....77
   APPENDIX B. VELOCITY DERIVATIONS....82
   APPENDIX C. HARDWARE TESTS....92
   APPENDIX D. STEERING ARC DERIVATIONS....99

APPENDIX E. DATA FROM TEST #1.....104
APPENDIX F. FREQUENCY COUNTER SPECIFICATIONS.....112
APPENDIX G. OPTICAL ISOLATOR CHIP SPECIFICATIONS.....118
APPENDIX H. MULTIPLEXOR CHIP SPECIFICATIONS.....120
APPENDIX I. ENCODER SPECIFICATIONS.....122

VITA.....125

LIST OF FIGURES

FIGURE PAGE

2.1 Wheelbase of the CGV showing the steering axle and encoder locations.....5

2.2 Block diagram of the conceptual operation of the CGV control scheme.....7

2.3 Block diagram showing the CGV equipment interface.....9

2.4 CGV sideview with structural parts and equipment.....10

2.5 Frontview of the CGV.....11

2.6 Diagram of the CGV control circuit.....16

2.7 Block diagram of the CGV control circuit operation for the encoders and the DC motor.....17

2.8 CGV wheelbase dimensions (inches).....21

2.9 Rearview of the CGV.....25

3.1 CGV following a straight line path.....33

3.2 Block diagram demonstrating the correction angle control scheme.....35

4.1 Initial CGV alignment for all straight line paths....42

4.2 CGV straight line path test #1.....44

4.3 Test path #1 as calculated from the encoder data.....46

4.4 CGV straight line path test #2.....47

4.5 Test path #2 as calculated from the encoder data.....49

4.6 CGV stability simulation with Θ_{max} = 0.004 radians....51

4.7 CGV stability simulation with Θ_{max} = 1 radian.....53

4.8 Calculated path from the encoder data with Θ_{max} = 1 radian.....55

5.1 Encoder-1 data from straight line test #1.....58

5.2 Encoder-2 data from straight line test #1.....59

FIGURE PAGE

5.3 Steering corrections performed for straight line test #1.....60

5.4 Encoder-1 data from straight line test #1 plotted with its running average.....62

5.5 Encoder-2 data from straight line test #1 plotted with its running average.....63

5.6 Encoder ratios with $F_2 > F_1$.....65

5.7 Encoder ratios with $F_1 > F_2$.....66

B.1 Wheelbase of the CGV showing the symbols used in the velocity derivations.....84

D.1 Wheelbase of the CGV showing the symbols used in the derivations for the steering arc.....101

CHAPTER 1

INTRODUCTION

1.1 BACKGROUND

Automated Guided Vehicles (AGV) are often employed in industrial settings to move materials from one location to another. Loads the AGV's are required to carry are dependent upon the nature of the task they are to perform. The one function that all AGV's have in common is they must be able to move from one location to another without the benefit of human feedback. Remote signals, electric wires, cables, and magnetic strips mounted in or on the floor are the most common methods that are used to guide AGV's. The installation of these guidance devices is fairly simple. However, if a new path or a variation of a path already in use is desired; more cables, wires, or strips must be put in place and the original placements must be taken up. It is this problem that is the catalyst for this thesis, the prototyping of a self-correcting, non-externally controlled computer-guided vehicle (CGV). The CGV operates by relying on a programmed path to control its direction. Wheels, referred to as tracking wheels, are in contact with the floor surface at all times. These tracking wheels are used to turn two optical encoders. The optical encoders through the use of a frequency counter yield

the CGV velocity information which is then integrated to determine the CGV's position. From this position information steering corrections are performed to keep the CGV on the desired path. Thus, the conceptual idea of the CGV's operation is based on using a pre-programmed path and velocity feedback from the encoders.

1.2 OBJECTIVES

The CGV should be able to follow a pre-programmed path in accordance with specified physical constraints, such as path length, path width, and turning locations. An advantage of this type of vehicle is the simplicity with which a path can be altered or created without the need to perform any physical modifications. The primary goal of this study is to determine the feasibility of the concept used to control the CGV. Some secondary goals are: 1) flexibility in the types of paths that can be programmed, 2) reduction of electrical and mechanical failures, 3) ability to operate on any reasonably smooth surface, 4) simple operation, 5) use of limited amount of hardware, 6) and low cost.

1.3 SCOPE

The scope of this study will be limited to the feasibility of the control scheme used to guide the CGV. An

evaluation of the performance of the CGV is discussed based on tests that give insight as to the ability of the CGV, its limitations, and parameters which affect its performance. Finally, recommendations are given concerning the CGV's performance and the feasibility of the presented guidance scheme.

CHAPTER 2

PROTOTYPE OVERVIEW

2.1 CGV OPERATION OVERVIEW

One of the goals in the CGV design was to have a vehicle that required very little input from a human operator to carry out a specified path. To help simplify the use of the CGV limited analytical methods have been developed to guide the CGV. Another aspect in the CGV's simplicity was the use of a limited amount of hardware to aid in the guidance scheme used to control the CGV. A control scheme was developed which would keep the CGV on a desired path by calculating a steering correction angle. This correction angle was based on the linear and yaw position of the CGV. The proposed control scheme involved the use of two encoders, one frequency counter, a lap-top computer, a stepper motor, and a DC gear motor. The encoders and frequency counter were used to determine the velocity of each end of the steering axle (see Figure 2.1). The steering axle was an imaginary axle passing between the two tracking wheels. Using these velocities, three independent first-order ordinary differential equations, which describe the X, Y, and yaw motion of the steering axle for different steering angles, were numerically integrated in real time to determine the position of the reference point of the

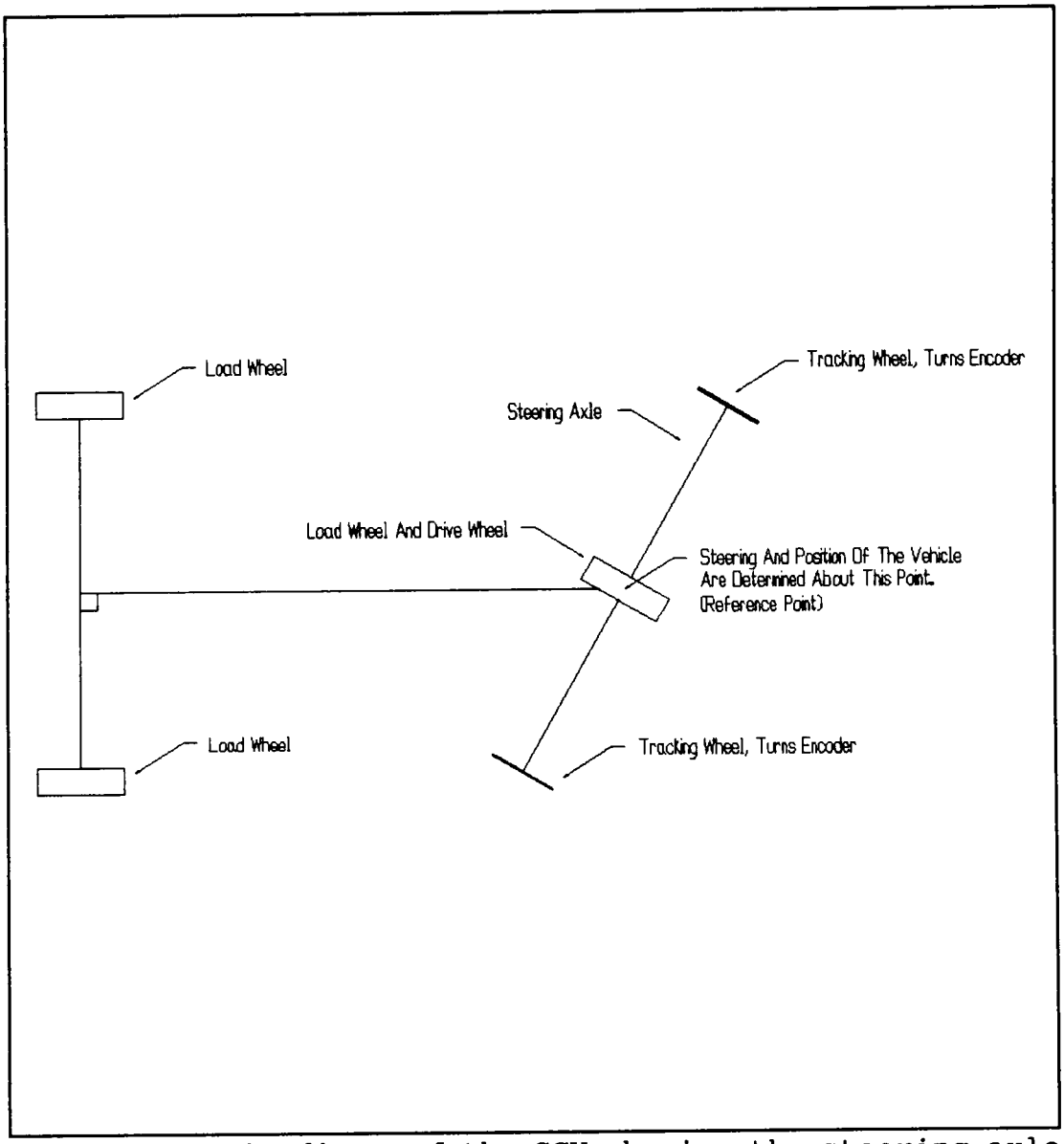

Figure 2.1: Wheelbase of the CGV showing the steering axle and encoder locations

vehicle. When the vehicle was found to be deviating from the desired path, steering corrections were made based on rotational and translational differences. An on-board lap-top computer carried out, in real time, all calculations concerning the path control of the vehicle. The computer also controlled all communication necessary to acquire the needed data in determining the vehicle velocity and direction control commands. The encoders were mounted on each end of the steering axle of the vehicle and would output signals only when the vehicle was in motion. A multiplexor was utilized to read the encoder signals by performing switching operations with proper commands through the computer's printer port. Each encoder signal was then interpreted by the frequency counter and with the use of the serial communications port, the computer received the necessary velocity data. A single stepper motor mounted on top of the vehicle performed all steering corrections by means of a double reduction. The final pulley ratio from the stepper motor to the steering was 25:1. These steering corrections were controlled by the computer through its printer port. A DC gear motor was used to drive the vehicle at an approximate constant velocity. The starting and stopping of the DC gear motor was governed by outputs through the computer's printer port. Figure 2.2 shows a block diagram of the CGV operation broken into its basic sequences. The velocity information received from the encoders was integrated to determine the position of the CGV. This position

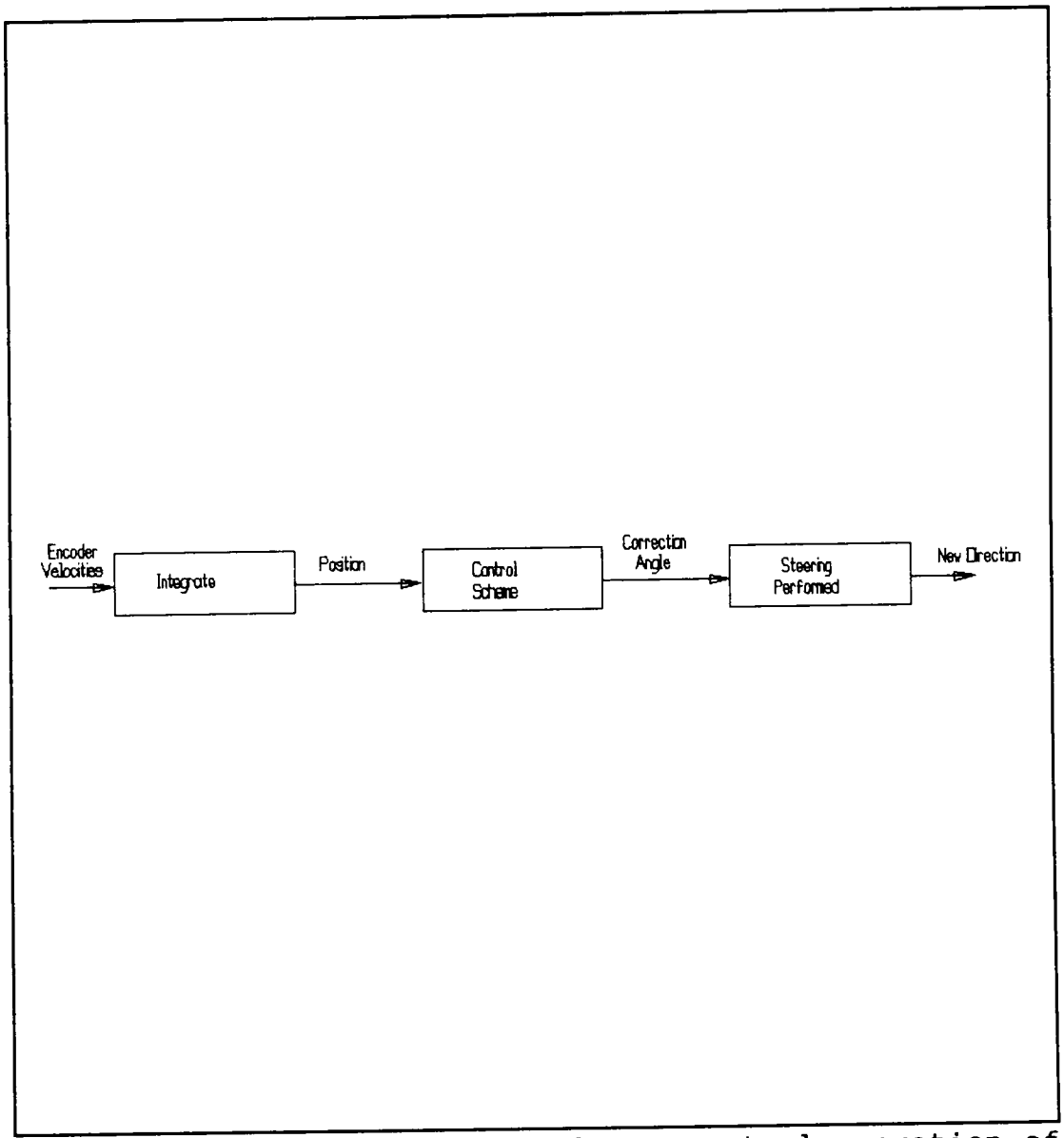

Figure 2.2: Block diagram of the conceptual operation of the CGV control scheme

information was then input to the CGV control scheme where the steering correction angle was then determined. The steering correction angle was then converted to a number of steps corresponding to how the stepper motor should be incremented. After the steering correction had been performed the CGV was then headed in a new direction where the same routine was repeated until the CGV run was completed. The overall control of the CGV was open-loop since the velocity data received from the encoders was taken as being absolute. In this vehicle design, there was no method by which the velocity data was checked to ascertain its accuracy.

2.2 PROTOTYPE EQUIPMENT AND OPERATION

The hardware chosen for the development of the prototype consisted of the following: a stepper motor, a stepper motor driver, a D.C gear motor, a laptop computer, a frequency counter, and two optical encoders. Figure 2.3 shows a block diagram of the CGV equipment and how it interacted. Notice that the laptop computer was the control center. Figure 2.4 shows a side view of the CGV. Some of the equipment and structural parts are labeled. Figure 2.5 is a front view of the CGV. The equipment and structure of the CGV shown in these figures is discussed in the following sections.

A 1.8 degree, 4.1 volt, 50 oz.-in. holding torque Step-Syn stepper motor was used to carry out all the steering

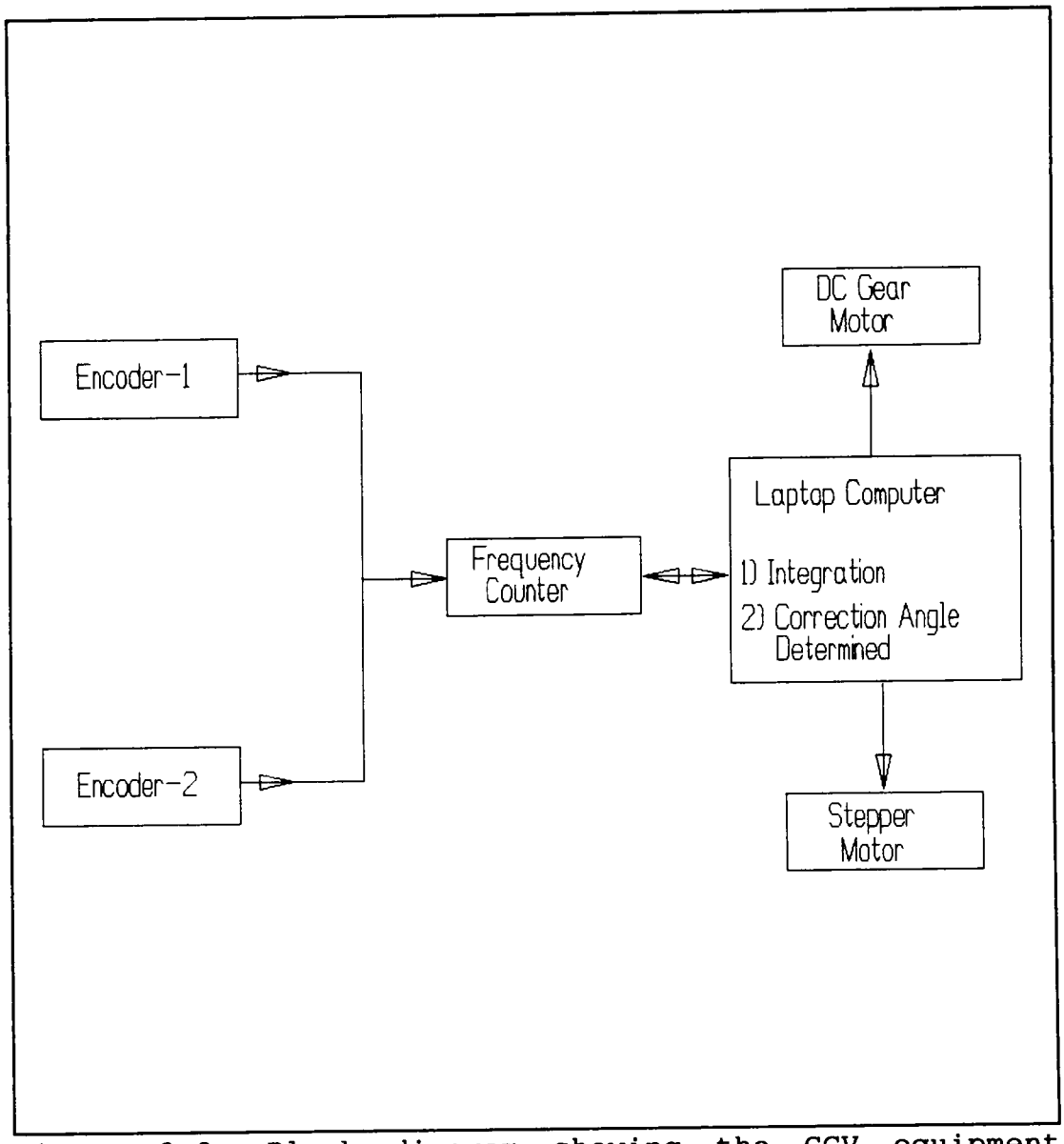

Figure 2.3: Block diagram showing the CGV equipment interface

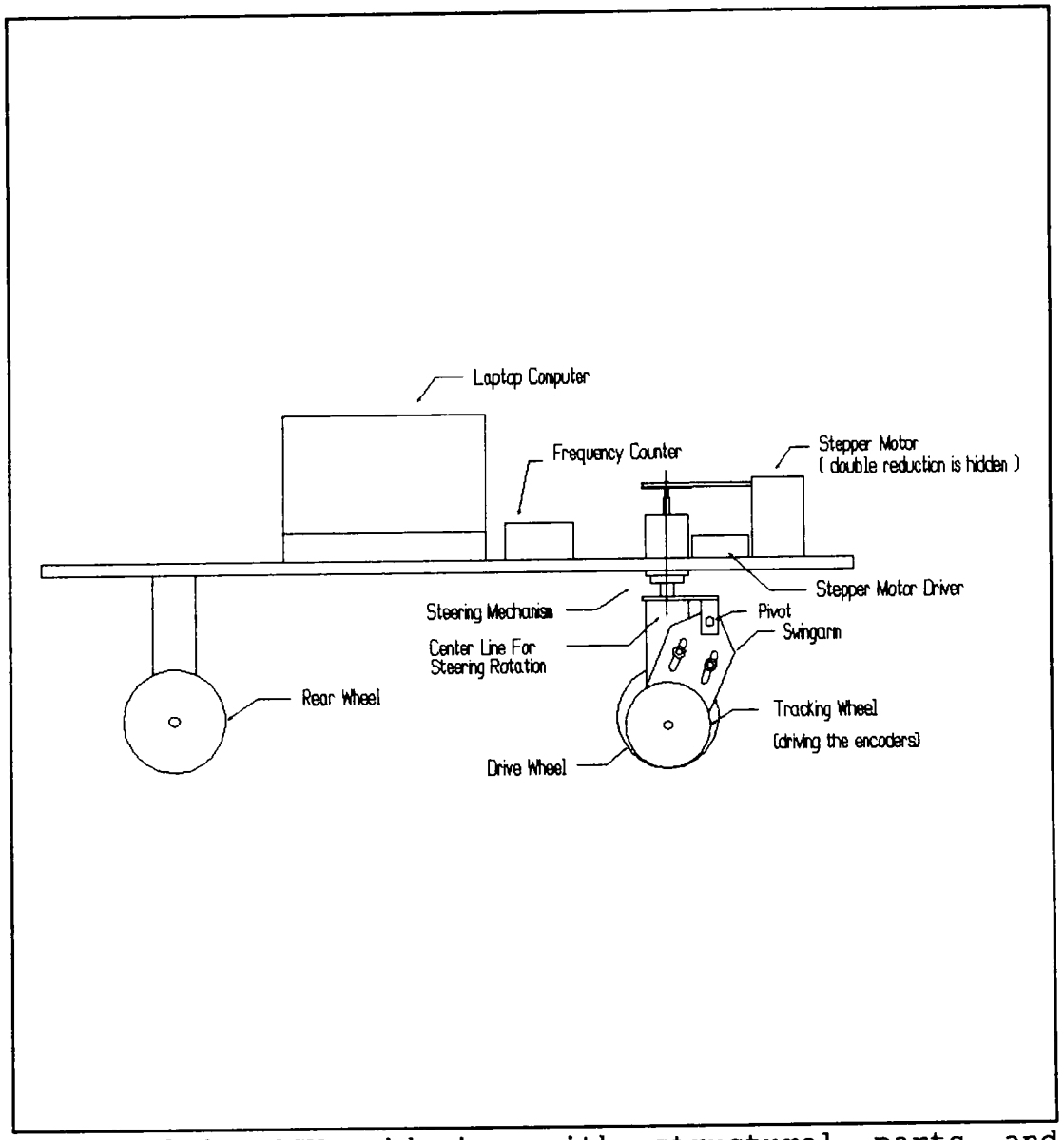

Figure 2.4: CGV sideview with structural parts and equipment

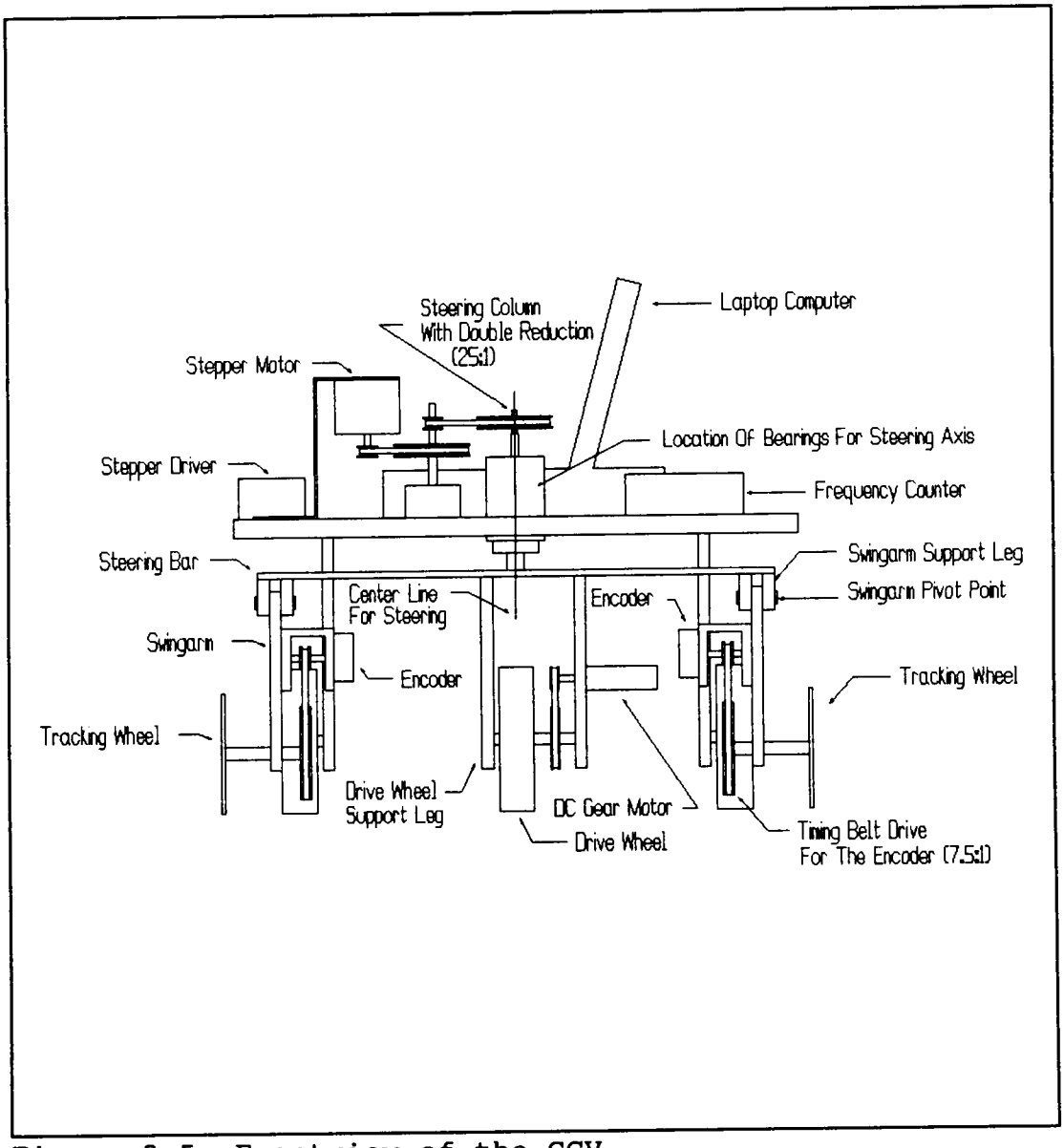

Figure 2.5: Frontview of the CGV

commands. A stepper motor was used to control the steering for several reasons. One, the incremental rotation of the stepper motor was easily controlled in open loop mode with the lap-top computer. Two, the stepper motor offers a sufficient torque output enabling it to accelerate the steering mechanism in a minimal amount of time. The stepper motor's holding torque allowed the proper steering angle to be held until the next steering correction was needed. An IMS IB463 stepper motor driver was used to drive the stepper motor. When a steering correction was needed the correction angle was converted from an angle to the number of steps corresponding to the direction and increments the stepper motor needed to be rotated. By using a For-Next loop in the computer code the number of steps needed to perform the steering correction was sent from the laptop computer to the stepper motor driver in a series of pulses. The stepper driver, in turn, sent pulses to the stepper motor corresponding to the pulse sent to the stepper motor driver. The information needed for incrementing the stepper motor was sent from the laptop computer to the stepper motor driver by way of the laptop computer's printer port.

A DC gear motor was used to drive the CGV forward at an approximately constant velocity (refer to Figure 2.5). During testing, the CGV was driven at a velocity of approximately 1.2 in/sec. By adjusting the input voltage to the DC motor the CGV's velocity could be changed. This ability to run the CGV at different linear velocities allowed for some

flexibility in the performance testing of the CGV. The on/off control of the DC motor was directed by outputs from the laptop computer's printer port. These outputs from the printer port served to open or close the DC motor circuit by way of a power MOSFET.

Two PMI M23 Modular Incremental Encoders were utilized to determine the linear, and rotational velocity of the CGV (refer to Figure 2.5). The encoders used were of high precision having 2540 pulse/rev. The CGV was tested at slow speeds which made the high resolution encoder better suited for low velocity measurements. As the CGV moved, the encoders generated pulses. The frequency of these pulses was directly proportional to the velocity of the CGV. The encoders were belt driven by 5 inch diameter tracking wheels. Using a ratio of 7.5:1 from the tracking wheels to the encoders, each encoder outputs 1,170 pulses/inch. The output frequencies from the encoders was a 12 volt CMOS compatible square wave and was input directly to the frequency counter. The optical encoders operate on a 12 volt power supply, and have a frequency response up to 100,000 hz.

One Acculex P6000 frequency counter was used to measure the frequency output of the encoders. The function of the frequency counter was easily controlled by the lap-top computer through its serial communication line. It was this ability to communicate with the computer and its compatibility with the encoder signal that made the frequency counter ideal

for this application. The P6000 frequency counter was fully programmable and had the ability to give frequency, frequency ratio, and totalizing pulse counts of the encoder signals. These varied functions of the frequency counter aid in the testing of the CGV hardware. The frequency counter was programmed prior to the testing of the CGV. Once programmed the frequency counter maintained its initial setup conditions. An external gate time was selected for the frequency counter. Gate time was the amount of time that the pulses from each encoder were averaged by the frequency counter. Because there was only one frequency counter, the encoders were each read at separate times by the frequency counter. This process required the ability to switch from one encoder signal to the other. A multiplexor chip was used to perform the switching operations. The multiplexor chip allowed the input signal to the frequency counter to be alternated from one encoder signal to the other. When each encoder signal had been averaged over the specified gate time, the frequency measurement was then input to the lap-top computer by way of the serial communications line. The communication line between the laptop computer and the frequency counter stayed open throughout the testing of the CGV.

2.3 PROTOTYPE CIRCUITRY AND OPERATION

The electronic system of the CGV was segmented into three areas. These involved the aspects of the CGV necessary for its proper control performance. The three areas were the steering control, DC motor control, and acquisition of the encoder readings. Figure 2.6 shows a schematic of the CGV circuitry and the laptop computer as the control source.

The first area of control was the steering of the CGV which involved the stepper motor/ stepper driver system. The laptop computer was responsible for all of the CGV control. The steering system was solely dependent on inputs received from the laptop computer. A BASIC For-Next loop was used to produce an alternating voltage at two pre-assigned printer port pins (0 and 1). This alternating voltage was then used to pulse the stepper motor driver. Each pulse the driver received was then used to energize (or de-energize) the stepper motor windings while in the half-step mode.

The second area of control was the operation of the DC gear motor. The best way to control the velocity of the CGV was to have independent control of the DC gear motor. The components used to control the DC gear motor were a power MOSFET, PS 2502 optical isolator chip, 4066 multiplexor chip, and the laptop computer. Figure 2.7 shows how the optical isolator chip and the multiplexor chip were utilized in the CGV control. An output through the laptop computer's printer

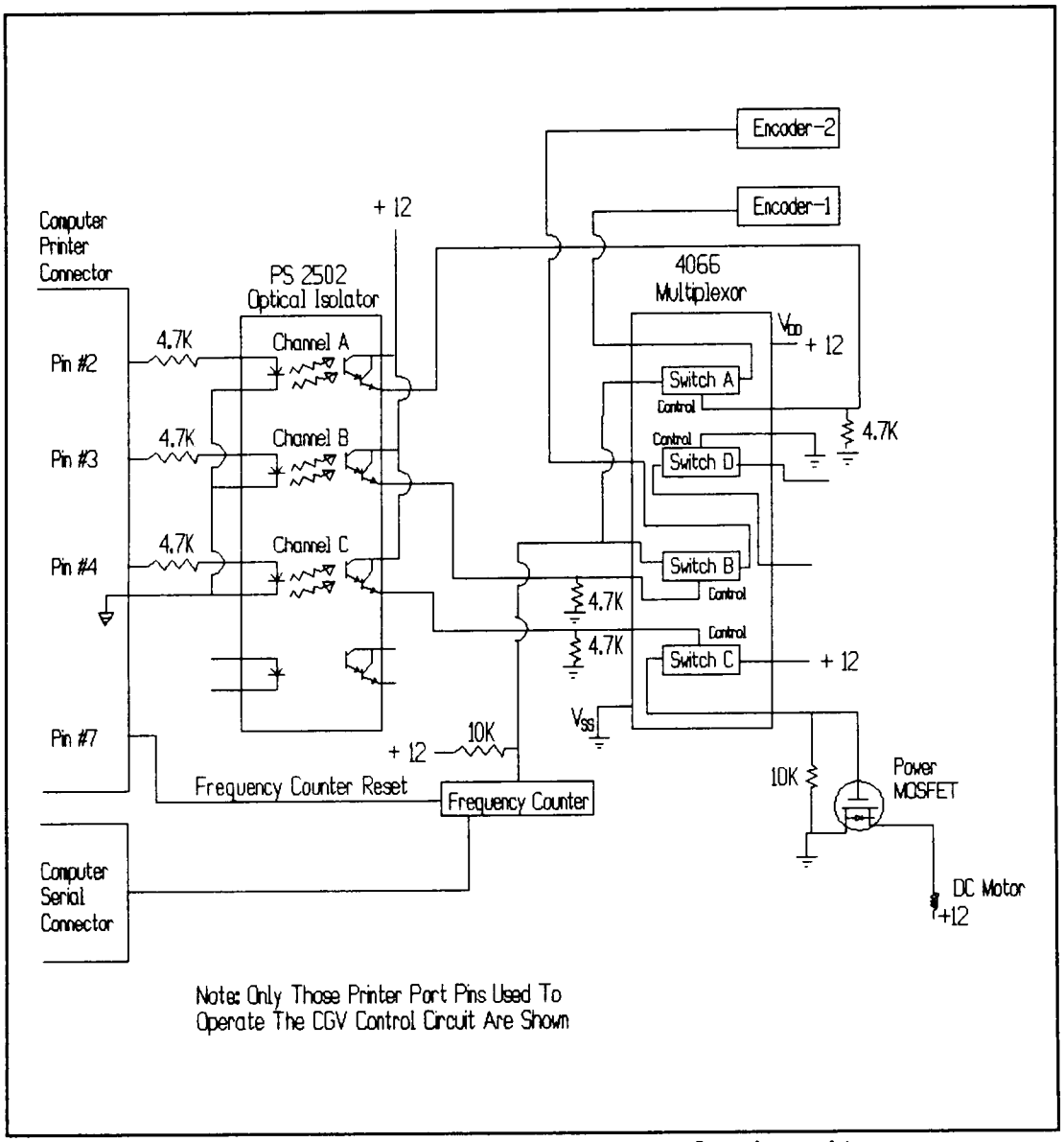

Figure 2.6: Diagram of the CGV control circuit

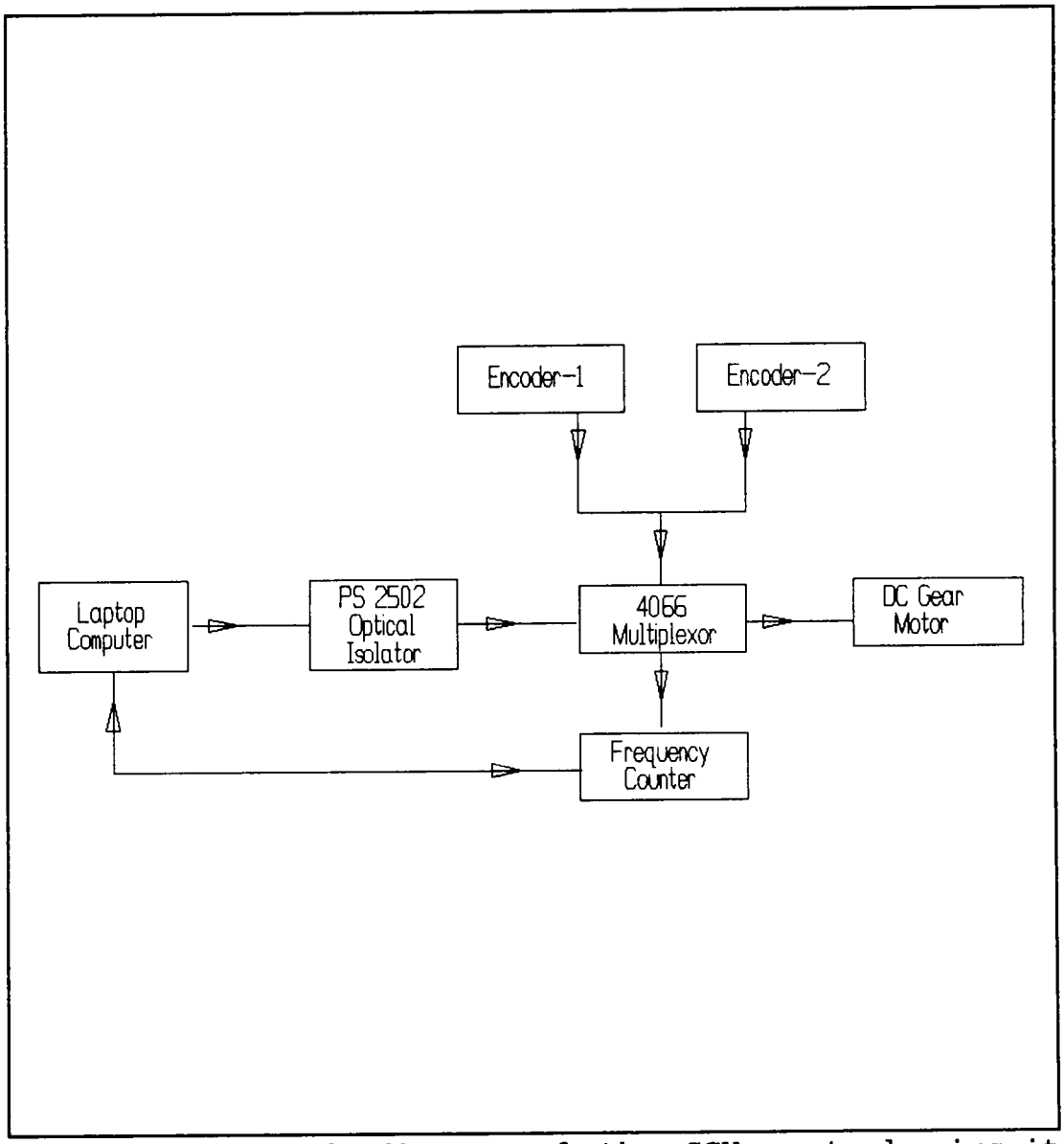

Figure 2.7: Block diagram of the CGV control circuit operation for the encoders and the DC motor

port pin #4 was used to induce a current in channel C of the optical isolator chip. When the switch in the optical isolator chip had been closed, current was allowed to flow to the multiplexor chip which in turn closed switch C. The power MOSFET controlled the current flow to the DC gear motor. When switch C in the multiplexor chip was closed, the 12 volt supply circuit to the DC gear motor was completed. Upon completion of this circuit the DC gear motor was operational. By adjusting the supply voltage to the power MOSFET the torque output of the DC gear motor could either be increased or decreased. At any point in the operation of the CGV the testing could be halted by proper inputs into the computer code controlling the CGV. This was accomplished by using a logic statement that looks for a keyboard command to stop the operation of the CGV. This keyboard command was the ESC key.

The third area of operation of the CGV was in the control of the velocity readings from the optical encoders (refer to Figures 2.6 and 2.7). Elements which were used in the collection of the velocity readings were the following; two optical encoders, a multiplexor chip, an optical isolator chip, a frequency counter, and a laptop computer. Both the optical encoders and the frequency counter shared a common 12 volt power source. However, each encoder was controlled by separate switches in both the optical isolator chip and the multiplexor chip. Each of these switches was controlled by a separate printer port of the laptop computer. During the

testing of the CGV it was necessary to read the velocity data from each of the encoders. Since only one frequency counter was employed, the signals that the frequency counter received from the encoders were alternated from one encoder to the other. The encoder outputs were each passed through separate switches in the multiplexor chip, switch A and switch B. The signal from encoder-1 was passed through switch A, and the signal from encoder-2 was passed through switch B. This circuit was necessary to keep the encoder signals isolated from one another. Once the encoder signals passed through the multiplexor chip, they shared a common input line into the frequency counter. Outputs from printer port pin #2 were used to control the velocity readings from encoder-1, and outputs from printer port pin #3 were used to control encoder-2. The manner in which the velocity data was gathered was similar to the DC motor operation. The output voltage from the printer port was used to close the appropriate channel in the optical isolator chip, which then closed the corresponding switch in the multiplexor chip. When one channel in the optical isolator was closed the other was automatically opened (due to the changing printer port command), thus preventing the carry over of one encoder reading into the other. Another key part in the velocity data collection was the necessity to purge the frequency counter of the previous velocity reading. This was a simple task which involved the use of the laptop computer's printer port pin #7 to reset the frequency counter between the

velocity readings of encoder-1 and encoder-2. The frequency counter had a reset input which upon receiving a low signal from the laptop computer would reset the frequency counter.

2.4 PROTOTYPE STRUCTURE AND OPERATION

The physical dimensions of the CGV's wheel base were arbitrarily chosen. Any physical size could have been used but would have to take into account the equipment that would be used and how the equipment would be transported. The dimensions of the CGV wheel base were the following: the length from the center point of the front drive wheel to the midpoint of the two rear wheels was 31.5 inches; the distance between the center points of the two rear wheels was 15.5 inches; the distance between the center points of the two tracking wheels was 24.25 inches; the distance from the floor to the top of the CGV was 13 inches. Figure 2.8 shows the CGV wheelbase with these dimensions.

The steering mechanism of the CGV consisted of the stepper motor, steering column, steering bar, and the front drive wheel (refer to Figure 2.5). The stepper motor was used to rotate the steering column by means of timing pulleys and timing belts arranged in a double-reduction scheme. The steering bar was attached to the steering column and was used to support the front drive wheel.

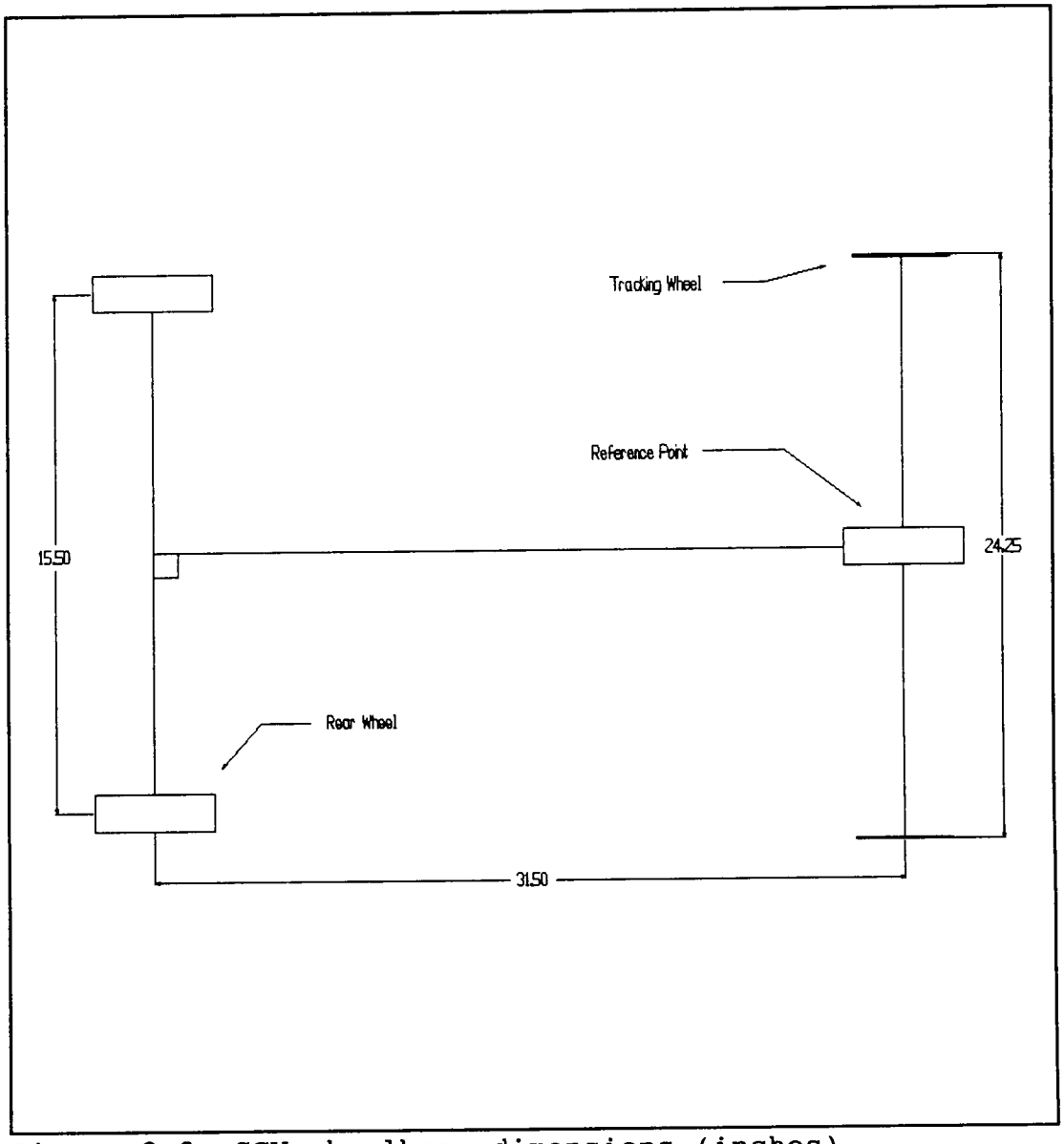

Figure 2.8: CGV wheelbase dimensions (inches)

From the stepper motor to the steering column there was a 25:1 reduction accomplished by four timing pulleys and two timing belts. This reduction served two functions. Without a multiplication in the stepper motor's output torque it would have been impossible to rotate the steering mechanism with the stepping motor. The needed torque to rotate the steering mechanism was 600 oz-in. The 25:1 reduction provided the necessary torque about the steering column to carry out all of the steering corrections. It was found through computer simulation of the CGV path that it would be necessary to provide the ability to perform small steering corrections. By operating the stepping motor in the half-step mode and having the 25:1 reduction, the resolution of the steering was 0.000628 radian/step. All of the steering and velocity information were related to the center point of the steering column (see the velocity analysis in Appendix B). The steering bar was rigidly attached to the steering column. The steering column consisted of a cylinder, one shaft, one angular contact bearing, and one ball bearing. The two bearings were used to prevent the axial and radial motion of the shaft. The steering bar was attached to the steering column shaft by a bolt which passed through a hole drilled in the steering bar into the internal threads of the shaft. The steering bar served two functions : it provided rigid support for the swingarms and the drive wheel (refer to Figure 2.5).

Swingarms are shown in Figures 2.4 and 2.5 and are located on the ends of the steering bar. Each swingarm had three functions: the encoders were mounted on the swingarms, the tracking wheels mounted to the swingarms, and both swingarms were allowed to pivot about a fixed point (refer to Figures 2.4 and 2.5). There were two swingarms fixed to the steering bar by means of two support legs and one shaft. Each swingarm was allowed to "swing" between the support legs about a common pivot point, which was provided by the shaft. The encoders were mounted to the side of the swingarms. Each tracking wheel was connected to the swingarm by way of a shaft passing through the tracking wheel and the swingarm. The purpose of the tracking wheel was to rotate the encoder. This was accomplished by using two timing pulleys and one timing belt with a 7.5:1 pulley ratio which allowed the encoder to rotate at a higher angular velocity. The tracking wheel was in contact with the floor surface and was allowed to rotate due to the friction force between it and the floor surface. Gravity was used to keep the tracking wheels on the floor surface. Thus, as the tracking wheel caused the encoder to rotate, the encoder output a frequency that was proportional to the angular velocity of the tracking wheel. The swingarms were allowed to pivot to ensure that the tracking wheels were in contact with the floor surface at all times (accounting for the fact that no floor surface is perfectly flat). Both the encoder and tracking wheel timing pulleys were mounted to the

swingarms. This attachment keeps the pivoting of the swingarms from affecting the encoder readings by preventing any relative motion between the swingarms and encoders.

The drive wheel system was comprised of two drive wheel supports, one drive wheel, one DC motor, and a timing belt arrangement (refer to Figure 2.5). Each drive wheel support was rigidly mounted to the steering bar. The drive wheel was mounted between the two drive wheel supports by a shaft passing through the two supports and the drive wheel. A DC motor was used to rotate the drive wheel by use of a timing belt reduction, the drive wheel is 6 inches in diameter. A measured force of 6 pounds was needed to move the CGV linearly, which equates to a required torque about the drive wheel shaft of 18 lb-in. to move the CGV. The stall torque of the DC motor was 11 lb-in. By using a 4:1 reduction from the drive wheel shaft to the DC motor shaft the necessary torque to operate the CGV was provided. The drive wheel system operated independent of the stepper motor.

The rear portion of the CGV was comprised of two rear support legs, two wheels, and one axle. Figure 2.9 shows the structure of the CGV's rear portion. Both rear support legs were mounted rigidly to the top of the CGV, with the rear axle passing between the two support legs. The rear wheels were mounted on the rear axle on the outside portion of the rear support legs. Each rear wheel had a set of ball bearings fixed into their structure allowing the wheels to rotate

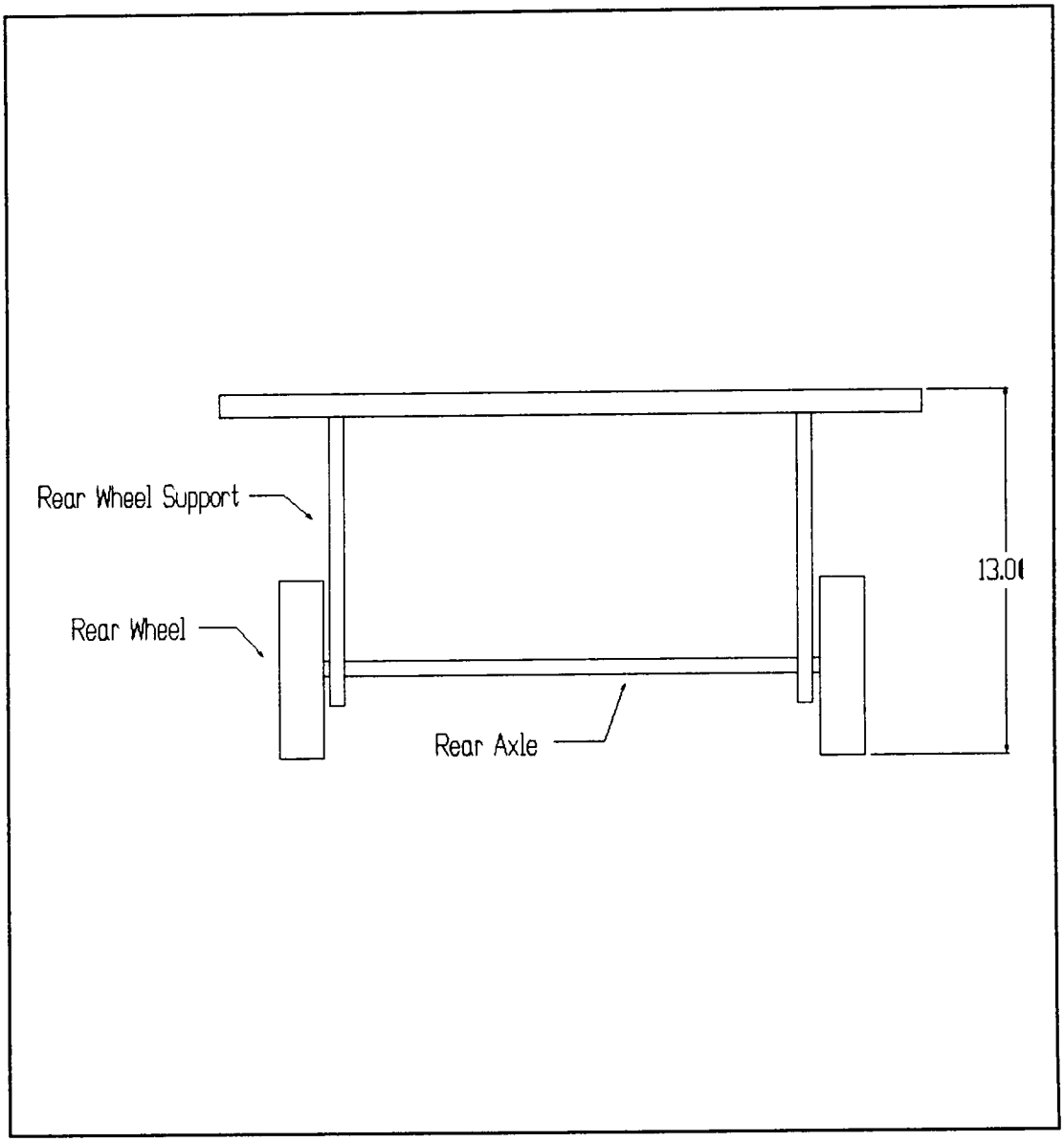

Figure 2.9: Rearview of the CGV

freely about the fixed rear axle. It was necessary that as the CGV was operating that the rear wheels offered no interference in the CGV's movement. Thus if the rear end of the CGV were isolated it would be possible to rotate the wheels and axle about a common center point.

2.5 CGV OPERATION OVERVIEW

A brief summary of the operating procedure that was followed for a CGV test run follows. This summary includes the entering of the path functions, initial CGV alignment, and a description of the CGV computer code sequences. The operation of the CGV hardware and the control of the laptop computer are brought together in this summary.

The path the CGV is to follow was entered into the appropriate location in the computer code. This had to be done while operating the laptop computer in the Quickbasic screen editor. The path was entered as an analytical function with the Y distance as a function of the X distance of travel, Y(x). Any function which had this characteristic and could be differentiated with respect to X can be used. Trigonometric, polynomial, and line functions can be used if they meet the above criterion. Other methods could have been used to guide the CGV. However, for the feasibility study of the CGV design, only analytical functions were used to describe the path. The bounds of the path functions used needed to be within the

limits of the physical environment where the CGV was tested. A straight line function was entered as Y(x) = mX + b, where m was the slope of the path and b was the Y intercept. The next function to be entered was the slope of the path, or simply put the derivative of the path function, Y'(x). Thus, to alter a path only two changes were needed in the CGV code; the functions Y(x) and Y'(x).

The initial alignment of the vehicle in relation to a fixed X, Y Cartesian coordinate system is required. Upon starting, the CGV computer code prompted for inputs which described its initial alignment. Three parameters which were entered into the computer were the initial angle of the drive wheel (with respect to the X axis), the location of the front point of the vehicle , and the location of the rear point of the vehicle. Without this information the CGV would have had absolutely no knowledge as to its position. After this information was entered into the computer code there was a slight delay before the vehicle started its operation, this was necessary to allow all path correction parameters to be recorded and the initialization of the path correction scheme. After the delay was completed the computer was given a command to start the DC gear motor (this command was performed within the computer code). On initial startup of the vehicle, velocity data was not taken due to the fact that the vehicle needed time to accelerate to an approximate constant velocity. If the velocity readings were allowed to be taken during the

acceleration period the encoder readings would differ by as much as 50%, thus introducing error into the system. When full velocity had been attained (approximately 2 seconds) by the CGV the velocity readings were allowed to be input to the computer code by way of the frequency counter. By opening the laptop computer's serial communications port, the encoder readings were interpreted by the frequency counter while the CGV was in motion. However, before any of the encoder outputs were read by the laptop computer, the communication buffer of the laptop computer was purged of any previous information. Once the communications buffer was emptied, the velocity data from encoder-1 was read into the computer code by way of the frequency counter. The frequency counter was then reset to purge itself of the previous encoder-1 velocity data, then the information from encoder-2 was read into the computer code. After the velocity readings from encoder-2 were received the frequency counter was again reset. The velocity information the laptop computer received from the frequency counter was in the form of pulses per second and on reception into the algorithm was converted to radians per second. Three coordinates were used to describe the position of the CGV, X, Y, and yaw. The yaw described the rotation of the body of the CGV. The CGV's linear displacement was described by X and Y. With the angular and linear velocities of the CGV known it was then only a matter of integrating them to determine the amount the CGV had rotated and its linear progression. The total

angle of rotation was updated with each velocity reading, with respect to the inertial coordinate system. The linear displacement of the CGV was also updated after each velocity reading. The linear displacement was measured with respect to the initial location of the CGV (0,0). Linear displacement of both the front and rear points of the CGV were calculated. Once the present location of the vehicle was determined from the integrated velocity data, the future point where it was desired for the CGV to travel towards was determined. To direct the CGV towards this future point a steering correction angle was calculated. This correction angle took into account the present linear and angular location of the CGV. When the required steering correction angle was determined it was then necessary to send this information to the stepper motor driver, which in turn would pulse the stepper motor. The steering correction angle was converted to the number of steps the stepper motor needed to be incremented to perform the proper steering correction. When this information had been processed, the stepper motor was then incremented the proper number of steps in the correct direction. After the steering correction was performed, the angle that the steering mechanism was rotated was then added to the previous steering angle. The same procedure starting with the purging of the communications buffer was repeated for the operation of the CGV.

CHAPTER 3

CGV CORRECTION ANGLE CONTROL SCHEME

3.1 CONTROL SCHEME OVERVIEW

A closed-loop feedback system was used to control the steering output of the CGV. Based on knowledge of the CGV location, and the desired path direction and location, the error in the present location of the CGV was determined. The error in the CGV position was based strictly on the position information received by the laptop computer. The control scheme used in guiding the CGV was dependent upon three variables: the velocity information, the integration scheme, and the method used to calculate the steering correction angle.

The velocity information the laptop computer received from the encoders was the essential element in the control of the CGV. As shown in Figure 2.2 the velocity data was the first step in establishing the control of the CGV. If the velocity data was in error at any point, the guidance correction of the CGV would have been based on false information, possibly leading to increased deviations of the CGV from its pre-programmed path.

The integration scheme used to integrate the velocity data from both encoders was a factor which influenced

both the speed and the accuracy of the control scheme. At the start of the work a fourth order Runge-Kutta integration scheme was utilized to integrate the velocity data. However, it was discovered that the Runge-Kutta scheme would take too long to perform the necessary integrations. It was then decided to use an Euler type method of integration. Using Euler's method was done at a slight loss in accuracy but with a significant increase in speed. With this increased speed more integration steps could be performed per time, thus compensating for the reduced accuracy.

In the development of the control scheme, calculation speed was the most influential factor. The steering correction angle had to be analytically determined and implemented in a minimal amount of time. This minimal time was needed, due to the fact that the steering correction angle was determined between two specific points of location. If the CGV moved a significant distance before the steering correction took place, then the "proper" steering correction would have been performed at the wrong location. If the analysis in the calculation of the steering correction angle was time consuming, no matter how accurate it might have been, the control scheme would be inaccurate.

When the amount of time between steering corrections was large (greater than 2 seconds), two events occurred. The integration scheme would go unstable due to the large step

size, and the CGV would deviate considerably from the desired path before a steering correction was made.

3.2 CONTROL SCHEME DEVELOPMENT

The control scheme was based on the knowledge of the present location of the CGV and the location of the future point to correct towards. With these two points known, it was necessary to approach the desired future location in a "smooth" manner. The pivot point of the CGV steering was the reference point for all steering corrections. It was assumed that the CGV was never far off from the desired path giving the ability to perform small angles of correction. By using small correction angles it was possible to linearize the CGV's correction control scheme. The control scheme took into account the translational and attitude differences of the CGV's present location and its future location. The translational directions were measured with respect to an inertial X-Y Cartesian system with the steering correction angle measured relative to the X axis. Figure 3.1 shows an arbitrarily chosen heading for the CGV as it followed a desired straight line path. The control scheme obtains the steering correction angle from the feedback of the X, Y, and θ positions of the CGV. θ was the present angle of the CGV drive wheel with respect to the X-axis.

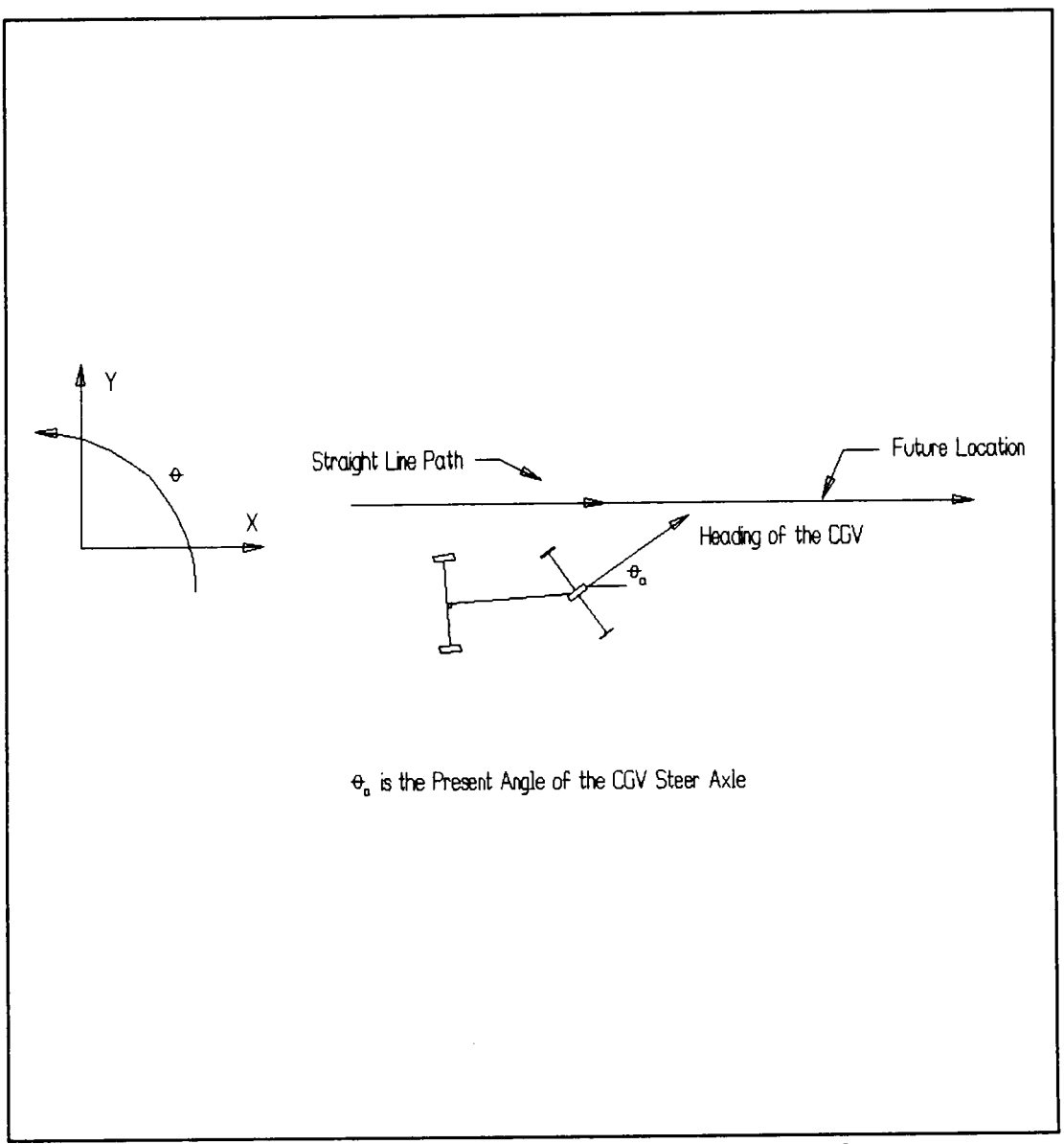

Figure 3.1: CGV following a straight line path

The steering correction angle for the Y feedback, Θ_y, was considered first. The part of the steering correction angle due to Y was obtained by feeding back the actual Y position of the CGV and obtaining the error given by the desired Y position minus the actual Y position. Figure 3.2 shows a block diagram of the control scheme used to determine the steering correction angle. In most control schemes this error would have been multiplied by a gain to obtain the steering correction angle. However, for the CGV a change in the steering angle also affected the X, and Θ positions of the CGV. As a result the Y feedback was multiplied by a weight function (W_y) which was a variable and dependent on the current CGV steering angle Θ_a. For example if the CGV was heading in the X direction but was off from the desired path by some ΔY, then a maximum value for the correction angle was needed to account for the Y difference. On the other hand if the CGV was heading strictly in the Y direction a minimum angle of correction was needed to account for the Y difference. It would then appear that a proper weight function needed the following characteristics. The weight function should be chosen such that for a small angle of Θ it would have a weight of 1 and for a value of Θ close to $\pi/2$ a weight which approached 0. The weight function also needed to be an even function of the angular direction of the CGV. This weight function allowed the sign of the Y difference to determine the correction angle sign. To satisfy these three criterion the

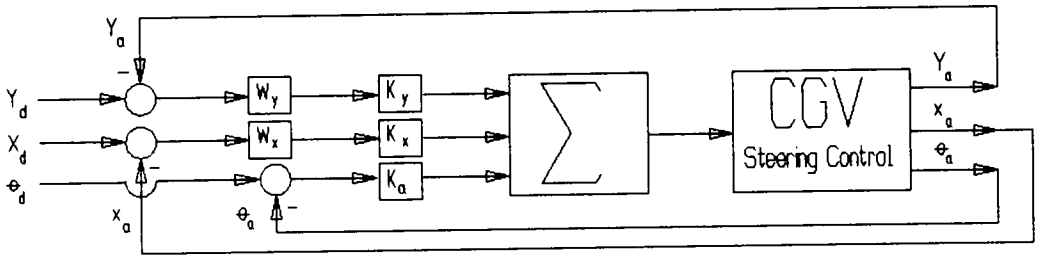

Y_a = Actual X Position of the CGV

X_a = Actual X Position of the CGV

θ_a = Actual Angle of the Steer Axle

Y_d = Desired Future Y Position of the CGV

X_d = Desired Future X Position of the CGV

θ_d = Desired Future Angle of the Steer Axle

K_y = Constant Gain for the Y Steering Correction

K_x = Constant Gain for the X Steering Correction

K_a = Constant Gain for the Attitude Steering Correction

W_y = Weight Function for thr Y Steering Correction

W_x = Weight Function for thr X Steering Correction

Figure 3.2: Block diagram demonstrating the correction angle control scheme

cosine function ($\cos(\Theta)$) was chosen as the weight function for the Y difference correction. Any function which satisfied the given characteristics for the weight function could probably have been used. Using $\cos(\Theta)$, the weight function for small values of Θ was a maximum; for large values of Θ it was a minimum and the cosine function was an even function of the angular direction of the CGV. If ΔY was large then Θ_y would also be large and the converse was also true. However, this ΔY feedback was modified by the weight function to reduce the feedback if the ΔY correction of the steering angle approached $\pm \pi/2$. In addition a constant gain K_y was used, and must be included in the correction angle to avoid instability. The final form of the feedback for the Θ_y correction angle was

$$\Theta_y = K_y \Delta Y \cos(\Theta_a) \qquad (3.1)$$

Notice the weight function was based on angles of Θ less than $\pm \pi/2$. This meant that the CGV steering angle would have to be aimed to within 90 degrees of the desired future point. Another property of the variable weight function was that it prevented the CGV from heading "backwards" if it was heading directly for the desired point.

The steering correction angle, component (Θ_x), for the X feedback was derived in the same manner as the Θ_y correction angle. The amount the CGV had deviated from the desired path in the X direction was obtained by subtracting

the actual X position of the CGV from the desired future X position. This value of ΔX was a linear feedback to the steering correction angle and was multiplied by a variable weight function. The characteristics of this weight function, (W_x), were the following. If the CGV was heading in the X direction the weight function should have a minimum value of 0, to minimize the steering correction. However, if the CGV was heading in the Y direction the weight function should have a maximum value which approached 1, to maximize the correction angle. The weight function also needed to be an odd function of the angular direction of the CGV. Using the sine function ($\sin(\Theta)$) as the weight function, these three criterion were met. For values of Θ which approached $\pm \pi/2$ the absolute value of $\sin(\Theta)$ was a maximum, and for values of Θ which approached 0 the $\sin(\Theta)$ was a minimum. A constant gain, $-K_x$, was used to add stability and influence the sign of the Θ_x correction angle. The final form of the contribution of the correction angle due to the X displacement was

$$\Theta_x = -K_x \Delta X \sin(\Theta_a) \qquad (3.2)$$

Again this weight function was based on angles of Θ less than $\pm \pi/2$.

The correction angle, Θ_{at}, for the attitude difference in the future and present location of the CGV was determined by the following. From knowledge of the CGV's

heading and the path direction the error in the angular position of the CGV was obtained. This error, $\Delta\theta$, was found by subtracting the present CGV heading from the desired future heading of the CGV. The $\Delta\theta$ feedback error was then multiplied by a constant gain, K_a, to obtain the θ_{at} steering correction angle. The θ_{at} correction angle became,

$$\theta_{at} = K_a\Delta\theta \qquad (3.3)$$

The three correction angles were then summed together and a final correction angle, $\Delta\theta_{cor}$, for the control scheme was obtained

$$\Delta\theta_{cor} = K_y\Delta Y\cos(\theta_a) - K_x\Delta X\sin(\theta_a) + K_a\Delta\theta \qquad (4)$$

This value of $\Delta\theta_{cor}$ was then input to the CGV steering control to perform the necessary steering correction.

An assumption made in this control scheme was that the CGV would perform steering corrections on a point location. However, this assumption was only valid in the computer simulation. Whereas in actual motion the CGV traveled in an arc as the steering maneuvers were being performed. An analysis of this problem was performed and reasons for its exclusion from the physical testing of the CGV are outlined in Appendix D.

3.3 CGV STABILITY

Two parameters which were found to affect the stability of the CGV were the constant gain values (K_y, K_x, K_a) and a maximum steering correction angle. The maximum steering correction angle imposed a limit on how much the CGV steering could be corrected at any time. The constant gain values, and the maximum correction angle were based solely on the computer simulation results and the actual testing of the CGV. With both the gain constants and the maximum correction angle there was a window of operation. The computer simulation, although not affected by the physical environment, offered insight into possible problems the CGV might encounter in the test runs and a quick way to evaluate alternative approaches.

The use of a maximum steering correction angle was shown to be a necessary facet in the control of the path taken by the CGV. This need for a maximum correction angle was found through the computer simulation. It was found through actual testing and simulation results that the CGV could indeed go unstable in its steering correction. These instabilities were found to occur in two areas. The first was that of having too small a correction angle and the other was having too large a correction angle. A summary of the CGV stability results are discussed in section 4.4.

CHAPTER 4

PERFORMANCE TESTING OF THE PROTOTYPE

4.1 STRAIGHT LINE PATH TEST

The CGV was tested on its ability to follow a pre-programmed straight line path. There are three reasons for using a straight line path. First, the encoder velocity data received can be analyzed to determine if the velocity readings adversely affect the CGV's performance. From a theoretical standpoint, if the CGV is moving in a straight line, the velocity readings from each of the encoders will be exactly the same. Secondly, the straight line path steering corrections will be small in comparison to the maximum steering correction angle. Due to this only small correction angles will be required and the CGV will spend less time performing steering corrections. With less time being used to perform the steering corrections, the integration step size will be decreased. The smaller integration step size improves the accuracy of the integration scheme. Thirdly, straight line paths can be more easily compared than paths which are curved. Over long distances greater inaccuracies would exist in the physical layout of the theoretical curved path than with one which was straight.

4.2 TEST SETUP

The CGV was allowed to travel over a distance of at least 30 feet to test the effectiveness of the control scheme for a straight line path. The test path was set up with respect to a fixed X-Y Cartesian coordinate system. The centerpoint of the front drive wheel was located at point (0,0), and the rear point of the CGV was located at (-31.5,0). The initial steering angle, θ, for these tests was 0 degrees. It was found through previous testing that the CGV should be aligned with the initial slope of the programmed path. This helps to maintain small angles of correction from the beginning of the test run. A gate time of 0.5 seconds was used with the frequency counter. The constant gain values in the steering correction angle were all set equal to unity. A maximum correction angle of 0.025 radians was used. All of these values were determined through computer simulation and actual testing. The programmed test path was a straight line along the positive X axis with a slope of zero. Figure 4.1 shows the initial alignment of the CGV for a straight line path. The collection of data to determine the performance of the CGV was made when the CGV reached a state of consistent performance. The path of the CGV was traced on the test surface by using a colored marker attached to the vehicle. After each test run the path was studied and measured to determine the characteristics.

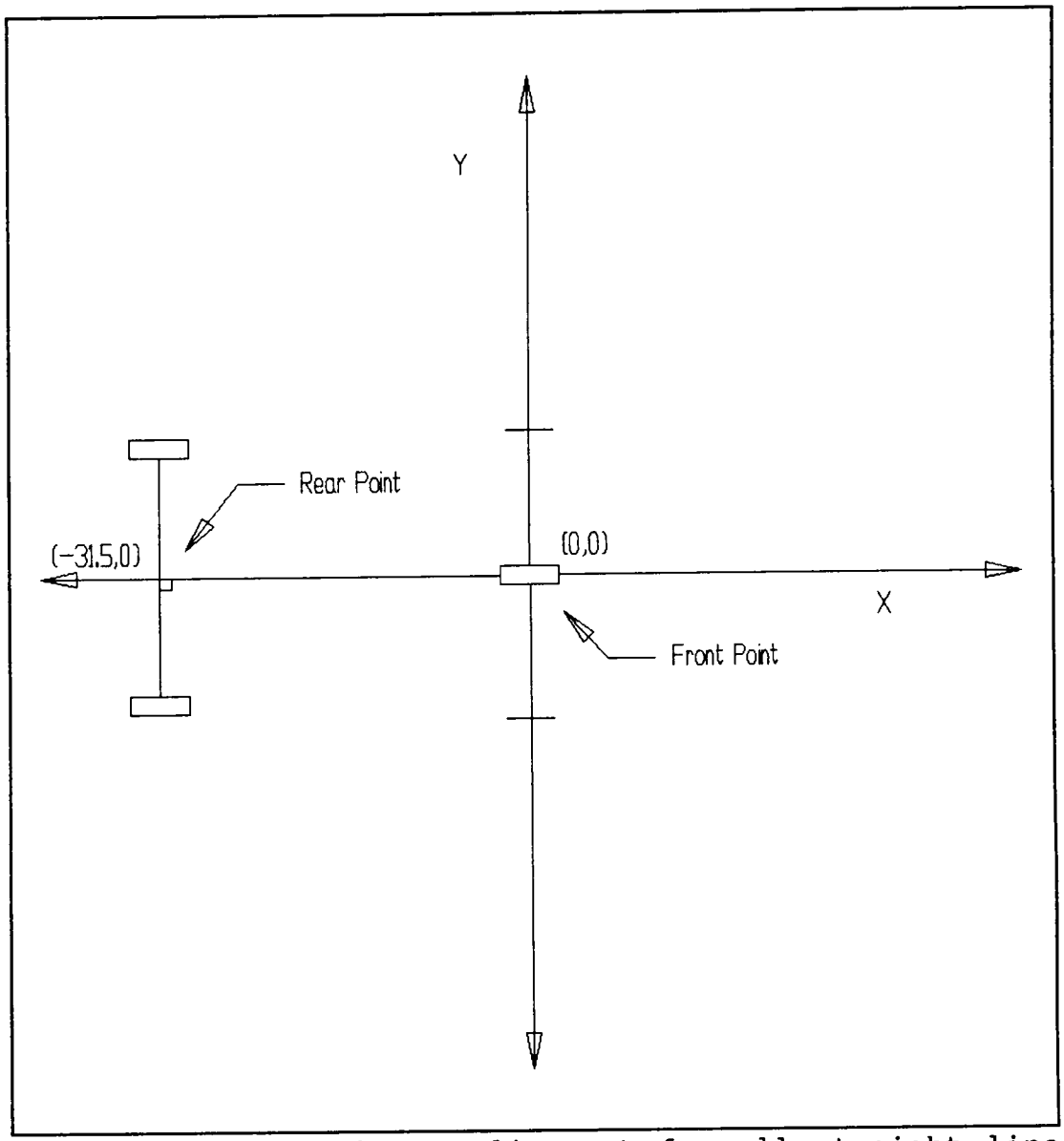

Figure 4.1: Initial CGV alignment for all straight line paths

4.3 DISCUSSION OF RESULTS

A plot of an actual CGV test run is shown in Figure 4.2. In Figure 4.2 different scales were used for the X and Y distances, due to the small change in Y when compared to X. The total length of the run was 405 inches with an average linear velocity of 1.23 in/sec. As can be seen from the Figure, the results of the test can be divided into five straight line segments. For example, the distance from point 1 to point 2 is considered one line segment. These line segments show a tendency of the CGV to deviate in the negative Y direction. It was observed that the line segments were not perfectly straight, but consisted of small oscillations (not shown in the figure) caused by the steering correction changes. These oscillations were predicted by the computer simulation model. As the CGV corrects itself it will go "left and right" about the programmed path as it makes corrections. If a straight line is drawn between any two successive points in Figure 4.2. the path traced by the CGV will be found to oscillate to the right and left of this line. There was never a case where the oscillations were either all to the right of this line or all to the left of this line. In Figure 4.2 the largest measured oscillation amplitude of any line segment from a straight line path was found to be between points 3 and 4 and was measured to be approximately 0.3 inches. The

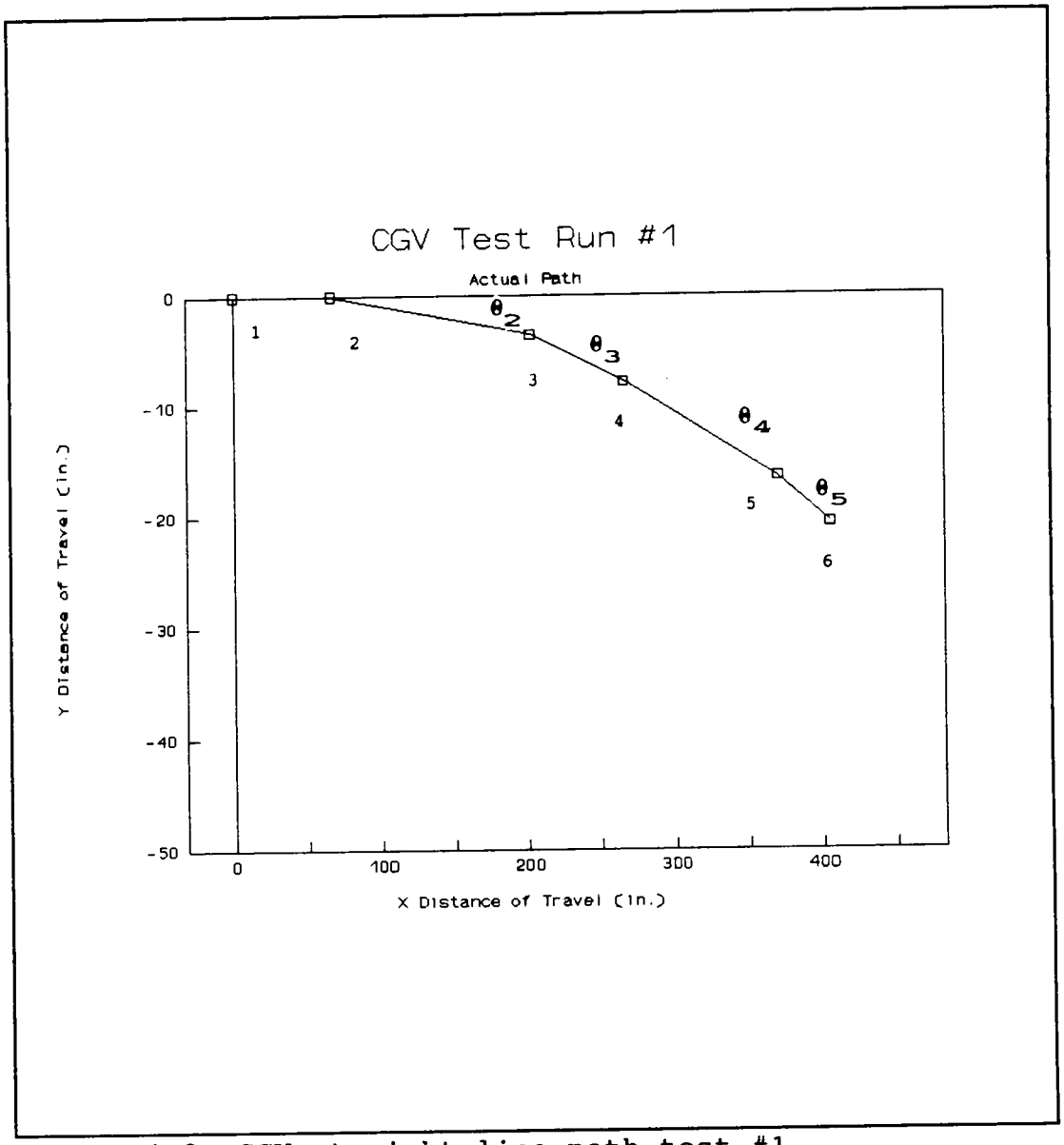

Figure 4.2: CGV straight line path test #1

oscillations for the other line segments were all measured to be approximately 0.25 inches.

Each line segment veers off from the previous segment in the negative Y direction at an angle, referred to as the deflection angle. The deflection angle is measured relative to the previous line segment. The maximum angle of deflection from the desired path was approximately 0.042 radians, which occurred at deflection angle Θ_3. Deflection angle Θ_2 was 0.026 radians, deflection angle Θ_4 was 0.016 radians, and deflection angle Θ_5 was 0.035 radians. The lengths and angles of these line segments were random in their magnitude and appearance. Figure 4.3 shows the computer code's interpretation of the path the vehicle was traveling during actual testing. From the computer data the maximum deviation of the CGV from a straight line was less than 0.1 inch. Although the actual path was not a straight line the computer gave data showing the path was essentially straight.

Figure 4.4 shows another test run plot of the path traced by the CGV. The total length of this path was 481 inches, with an average velocity of 1.26 in/sec. The same characteristics occur in Figure 4.4 as those shown in Figure 4.2. Each line segment was straight but with a variation in length, and each line segment was directed in the negative Y direction. The same oscillations occur in this path as were described in the previous path analysis. The maximum oscillation from the straight line path of any line segment

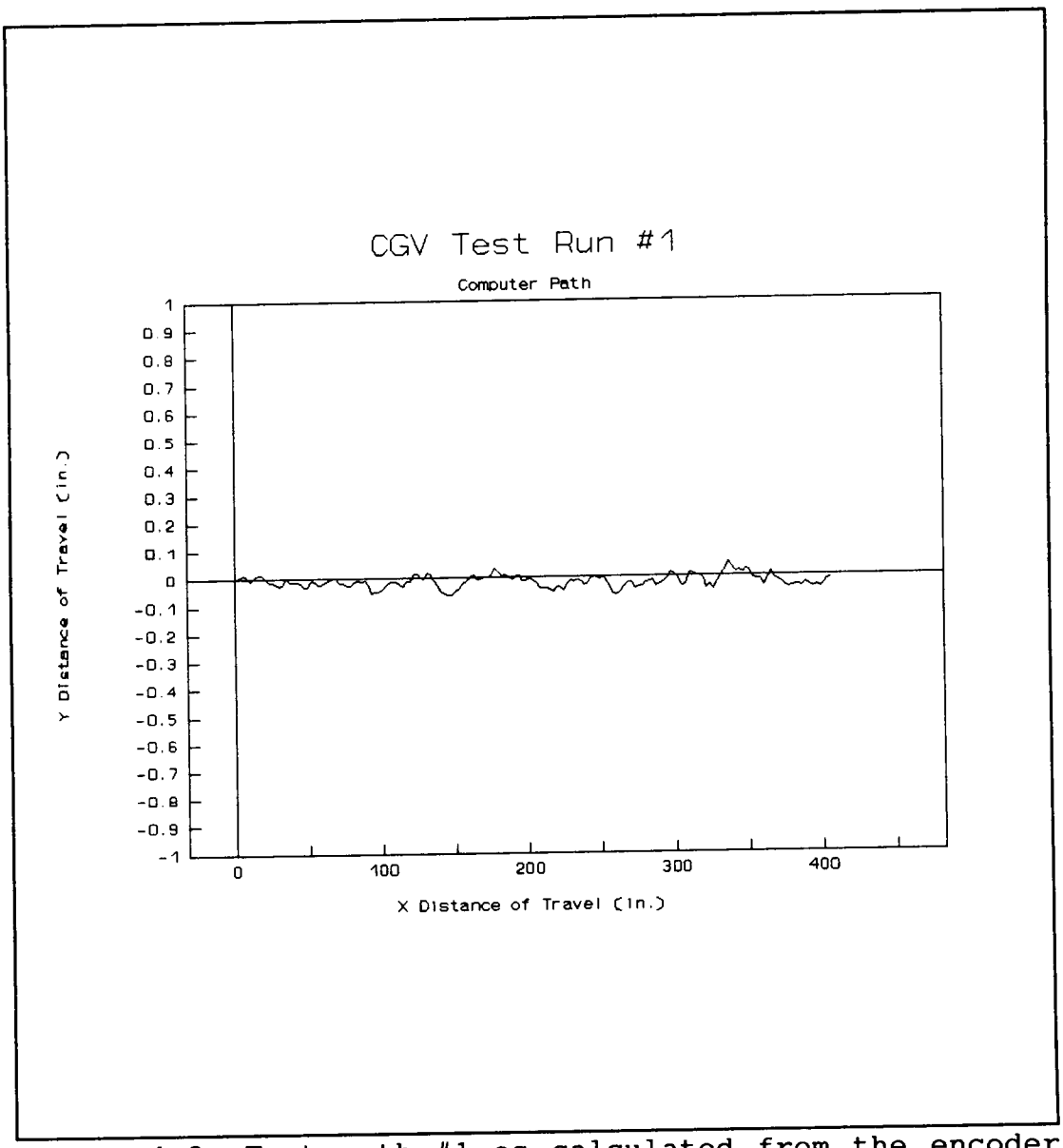

Figure 4.3: Test path #1 as calculated from the encoder data

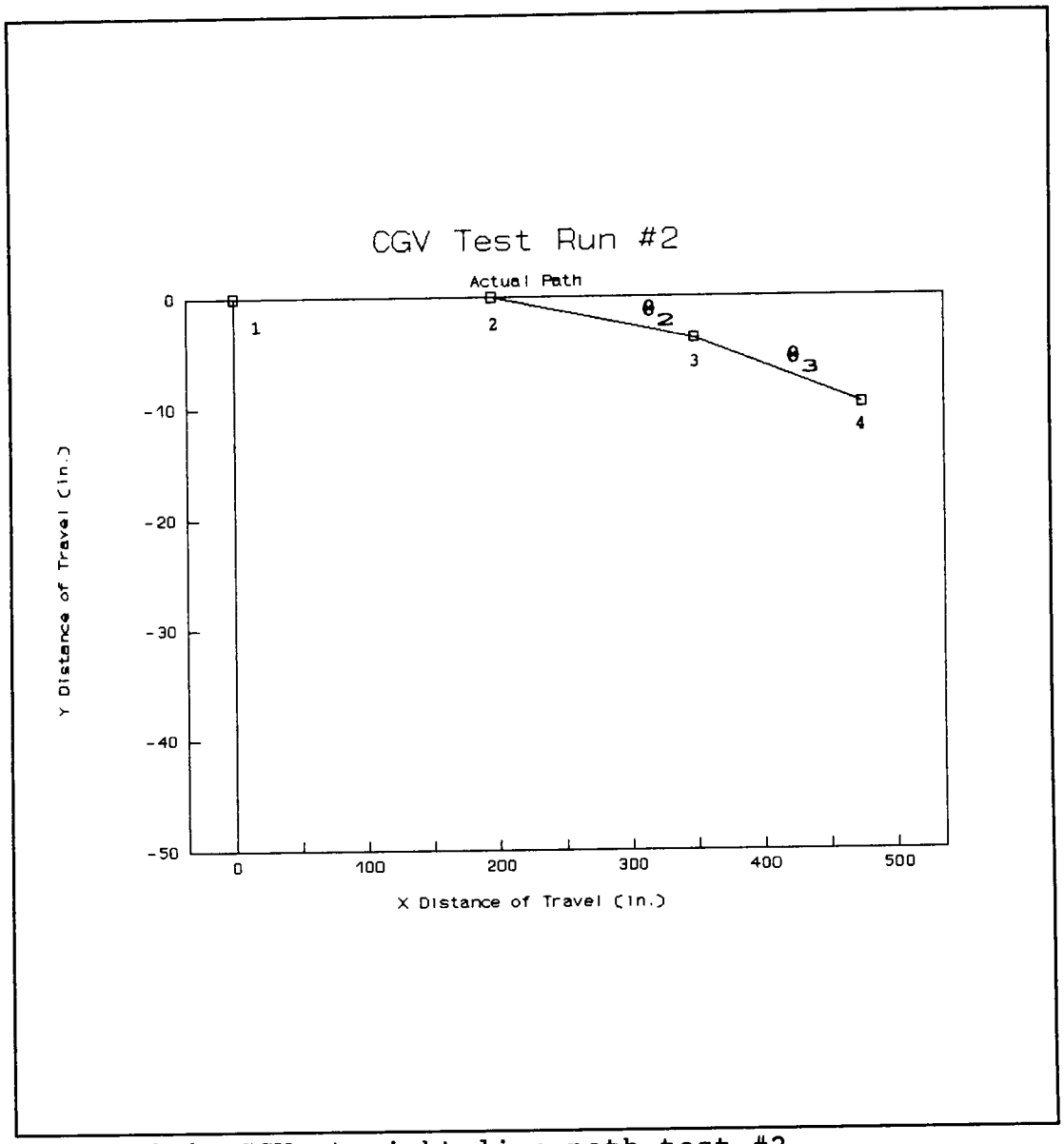

Figure 4.4: CGV straight line path test #2

was approximately 0.4 inches, occurring between points 3 and 4. The maximum angle of deflection was 0.024 radians at Θ_2, and deflection angle Θ_3 was 0.021 radians. Line segment 1-2 was the longest with a length of approximately 195 inches. A plot of the path the computer interpreted the vehicle was taking is shown in Figure 4.5. Again, according to the computer code, the CGV was traveling in a straight line.

These same performance characteristics were repeated in every test run of the CGV with a high level of consistency. The same test set-up conditions were used in all of the CGV tests, though in some tests parameters such as vehicle speed and frequency counter gate time were altered.

It was found during testing that linear velocities greater than 3 in/sec resulted in poor path corrections by the CGV. At the higher velocities, when the steering corrections were implemented, the CGV would travel a considerable distance due to the time between corrections. This distance could not be accounted for in the control scheme and caused the assumption of corrections performed on a point location to be no longer valid. The CGV essentially outruns the control scheme. All the data was collected at speeds near 1.25 in/sec.

A gate time of 0.5 seconds was used in all the presented results. In the latter stages of testing a gate time of 0.25 seconds was used. Using a lower gate time reduced the integration step size from 1.9 seconds to 0.9 seconds. The results of these tests showed the same characteristics as

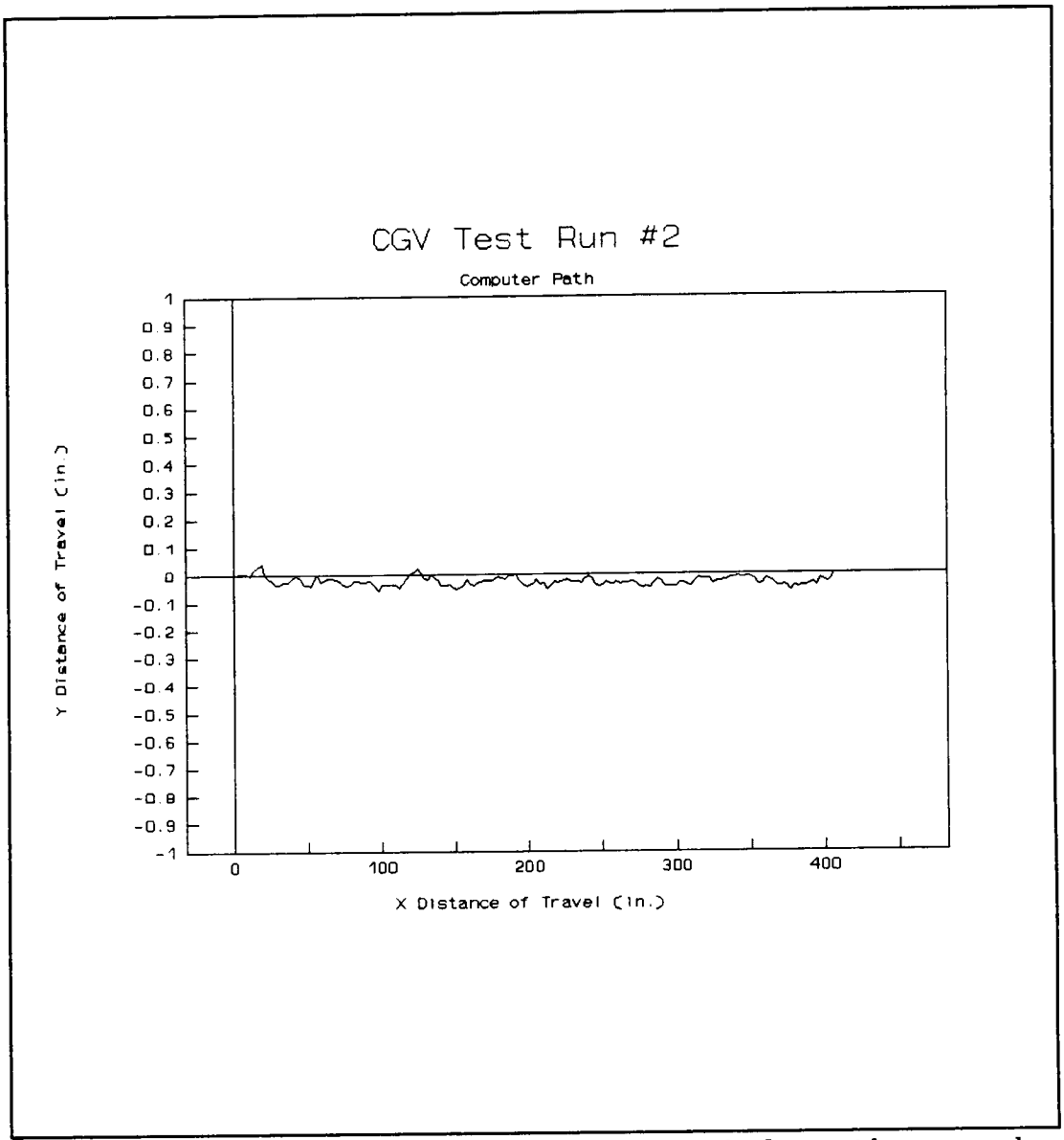

Figure 4.5: Test path #2 as calculated from the encoder data

those discussed previously. During the actual testing of the CGV higher gate times were used, but the increased averaging period of the velocity readings was offset by the increased integration step size. The larger step size reduced the accuracy of the integration scheme.

4.4 CGV STABILITY

As stated in chapter three, the CGV path is dependent upon the maximum allowed angle of correction. This maximum correction angle represents the most the CGV could be corrected at any one time. In the computer simulations for a straight line path, the maximum correction angle was tested at two extremes, one being "small" and the other being "large". During these computer simulations velocity data was generated by using velocity and time increment data from actual CGV tests. The time increment was approximately 1.9 seconds during which no simulated error was introduced. A maximum correction angle of 0.004 radians was used for the "small" extreme. Using this value in the straight line path correction, no signs of instability occurred. The CGV shows small oscillations with a maximum amplitude of 0.2 inches about the proposed straight line, Figure 4.6. The problem associated with using a correction angle which is too small is that the CGV will not be able to correct itself. If the path to be followed was curved the CGV will be unable to perform the proper steering

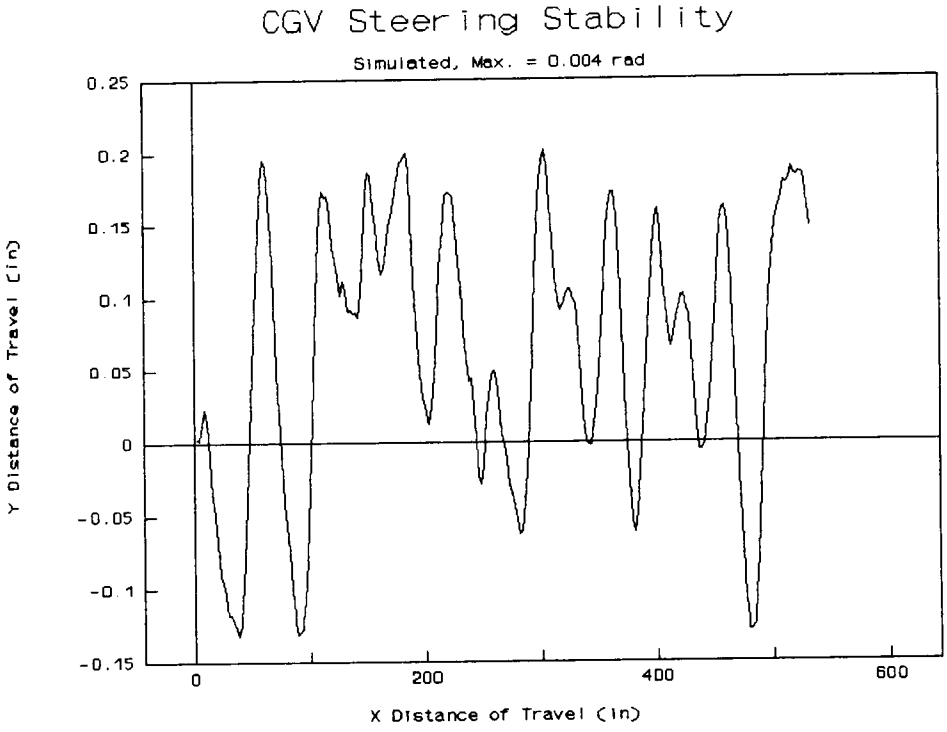

Figure 4.6: CGV stability simulation with Θ_{max} = 0.004 radians

correction to stay on the programmed path. The angle of correction would be too small to account for "large" differences in a path. In the simulation at the opposite extreme, a correction angle of one radian was used and is shown in Figure 4.7. The CGV has higher oscillations about the straight line path and shows no tendency to go unstable. However, it must be remembered that the computer can make corrections on a point and these corrections are transmitted instantaneously.

In the actual testing of the CGV each of the above correction angles were used. For the "small" correction angle (0.004 radians) the CGV displayed the same characteristics as in the previous path control discussions. It followed the path with no sign of instability. However, when the maximum correction angle of one radian was used, the CGV went unstable. Two major characteristics were displayed. One, the CGV went completely off path both physically and in the computer simulation. Two, the integration time increment increased to five seconds (and greater). With the steering angle increasing, the time to complete the steering correction also increased. This, in turn, increased the integration step size, completely eliminating any accuracy in the CGV path correction control scheme. The steering corrections gradually increased until they approached one radian. Eventually, the steering corrections alternated from one radian clockwise to

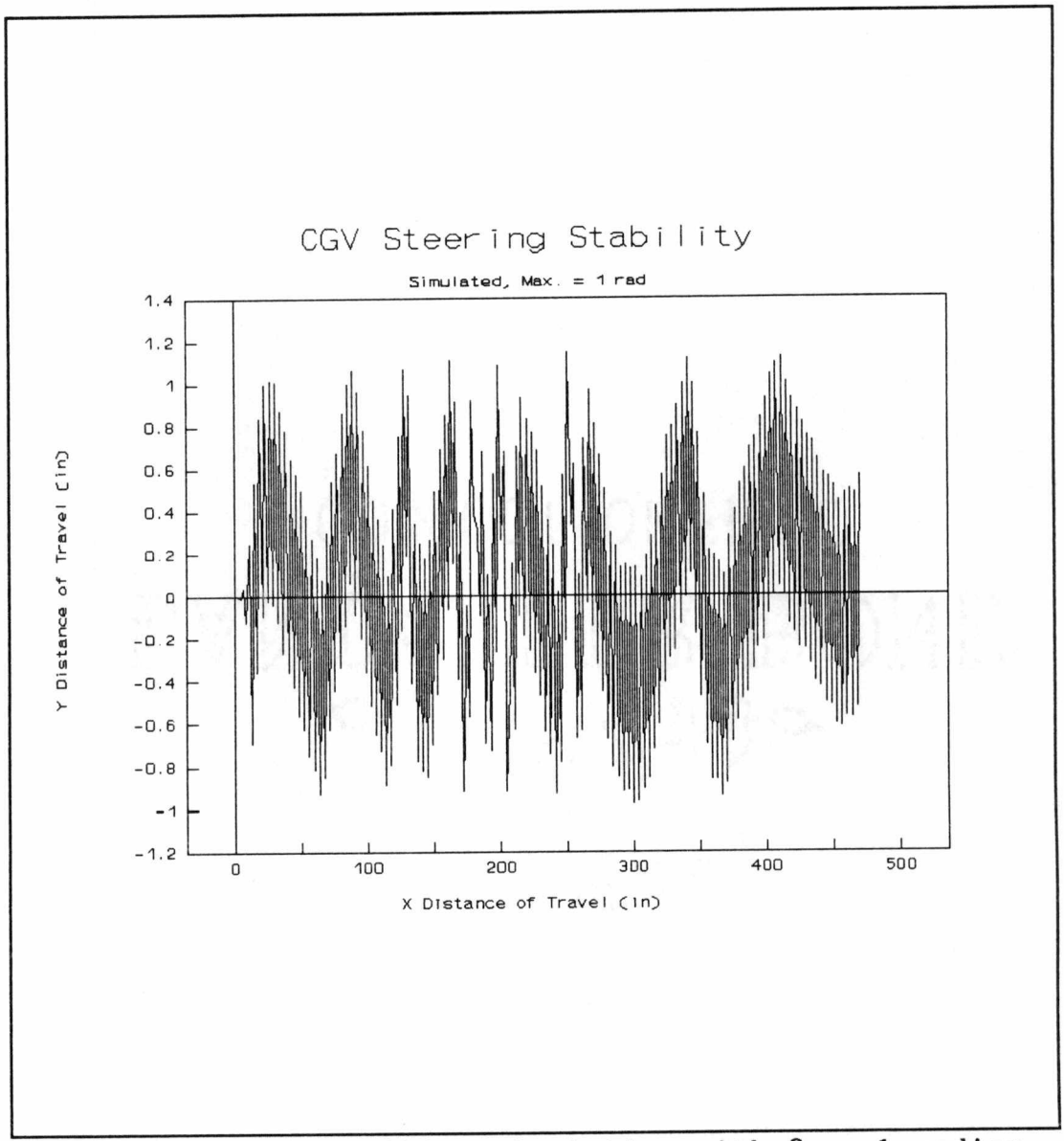

Figure 4.7: CGV stability simulation with Θ_{max} = 1 radian

one radian counter-clockwise. The path the computer interpreted the CGV was taking is plotted in Figure 4.8.

A maximum correction angle of 0.025 radians was used in the final data collection. This angle allowed the CGV to make a large enough steering correction to account for any deviation from the straight line path. Also, the time to perform this maximum correction angle took less than 0.3 seconds lowering the integration step size.

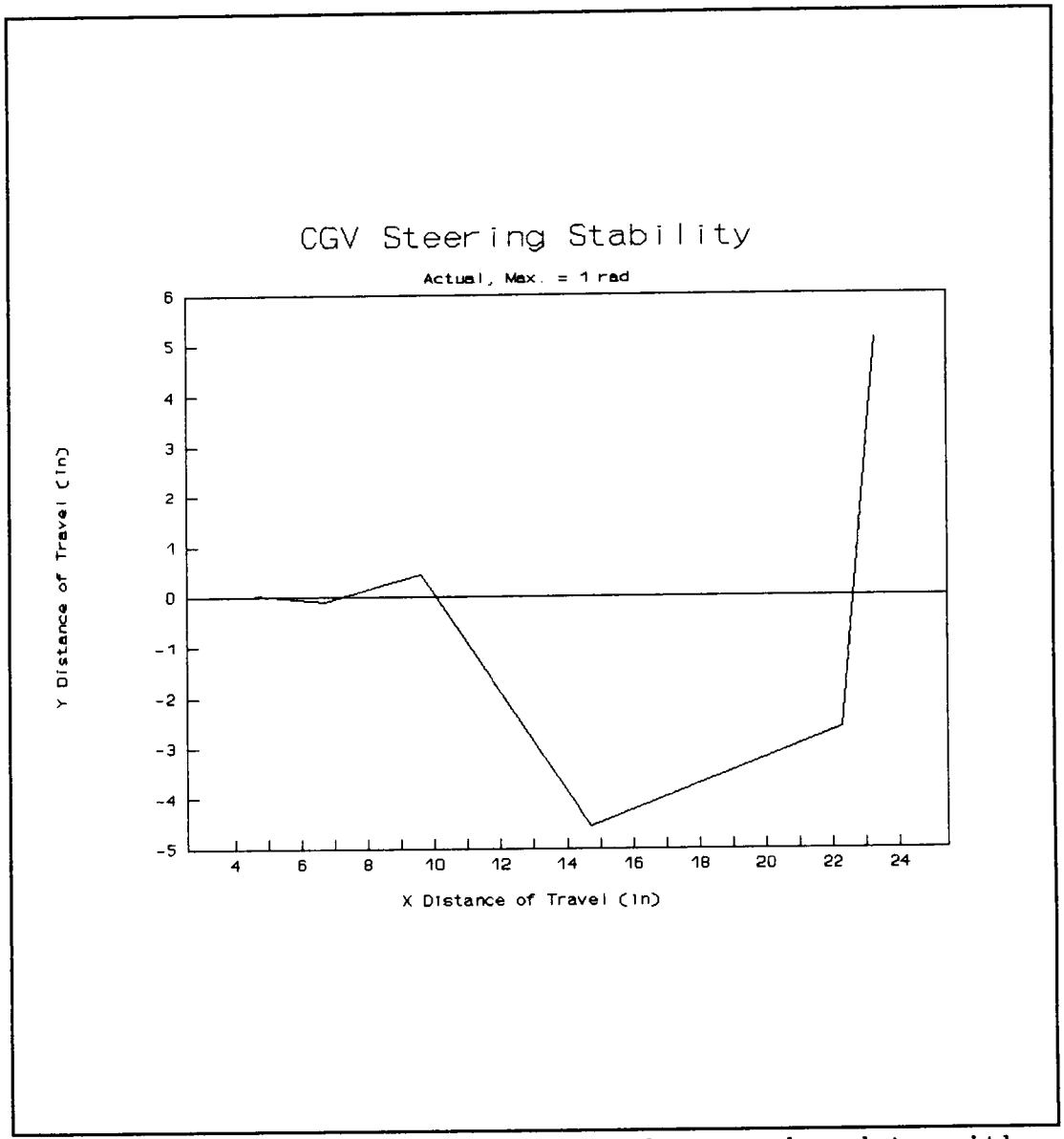

Figure 4.8: Calculated path from the encoder data with Θ_{max} = 1 radian

CHAPTER 5

DISCUSSION OF PROTOTYPE ERROR

5.1 ENCODER ERROR TESTS

Each part of the CGV hardware was tested independently to ascertain which individual piece of equipment, if any, was responsible for the performance problems of the CGV path control scheme. A detailed account of the test conditions and results is given in appendix C.

The analysis of the collected data showed the position error of the CGV was due to the error in the velocity data received from the encoders. Since all steering corrections are based upon the velocity data, any errors which may arise can be attributed to errors in the velocity data. Several tests were performed which gave support to this hypothesis. These tests included the actual test runs of the CGV, a running average of the velocity data, a constant steering angle test, and tests to calculate the radius of curvature of the CGV.

5.2 ACTUAL TEST RUNS

During each CGV data analysis, it was found that a series of negative steering corrections preceded locations

where the CGV deviated from the programmed path. These negative steering corrections were influenced by the encoder velocity data and caused the CGV to deviate in the negative Y direction. In each case of a series of negative steering corrections, there was a corresponding case of encoder-1 velocity readings being significantly higher than the velocity readings of encoder-2. The physical effect of encoder-1 being greater than encoder-2 is that the vehicle heads in the positive Y direction. The differences in the velocity readings caused the control scheme to make corrections to bring the CGV heading towards the X-axis. The difference in encoder velocities ranged from 4% up to 10%, where at the higher percent differences the physical effects were more easily distinguished.

A plot of each encoder's velocity data versus the X distance of travel is given in Figures 5.1 and 5.2. From these plots it is seen the velocity data was highly random. Also, from these figures the CGV's velocity is increasing and decreasing in magnitude. This changing velocity was observed during actual testing of the CGV. However, this is not a problem for the correction angle control scheme since it is capable of dealing with the changing velocity data. The collected data showed a large percentage difference in the encoder velocity readings before the negative steering corrections were made. Figure 5.3 shows a plot of the total steering corrections performed by the CGV. Initially the steer

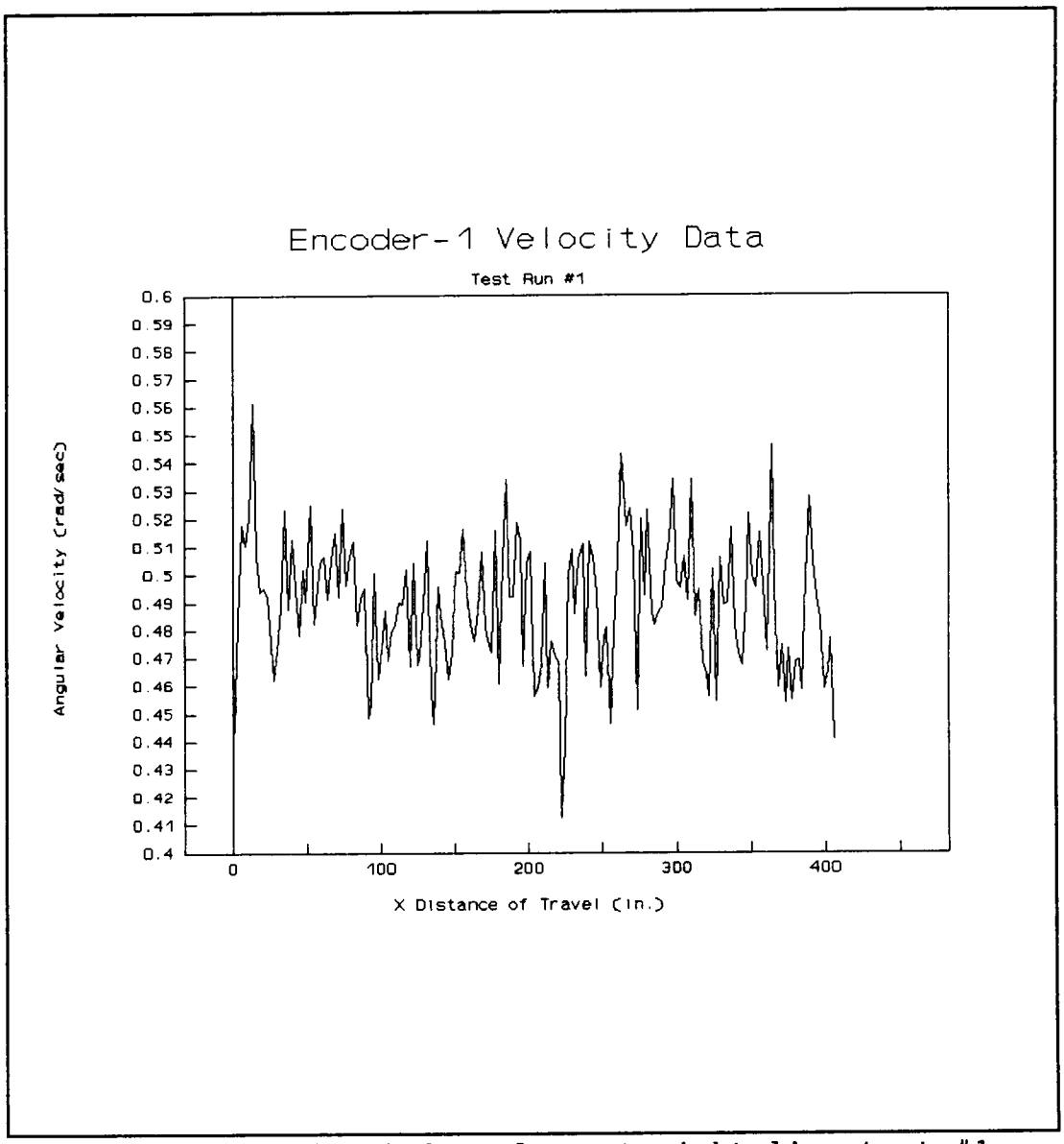

Figure 5.1: Encoder-1 data from straight line test #1

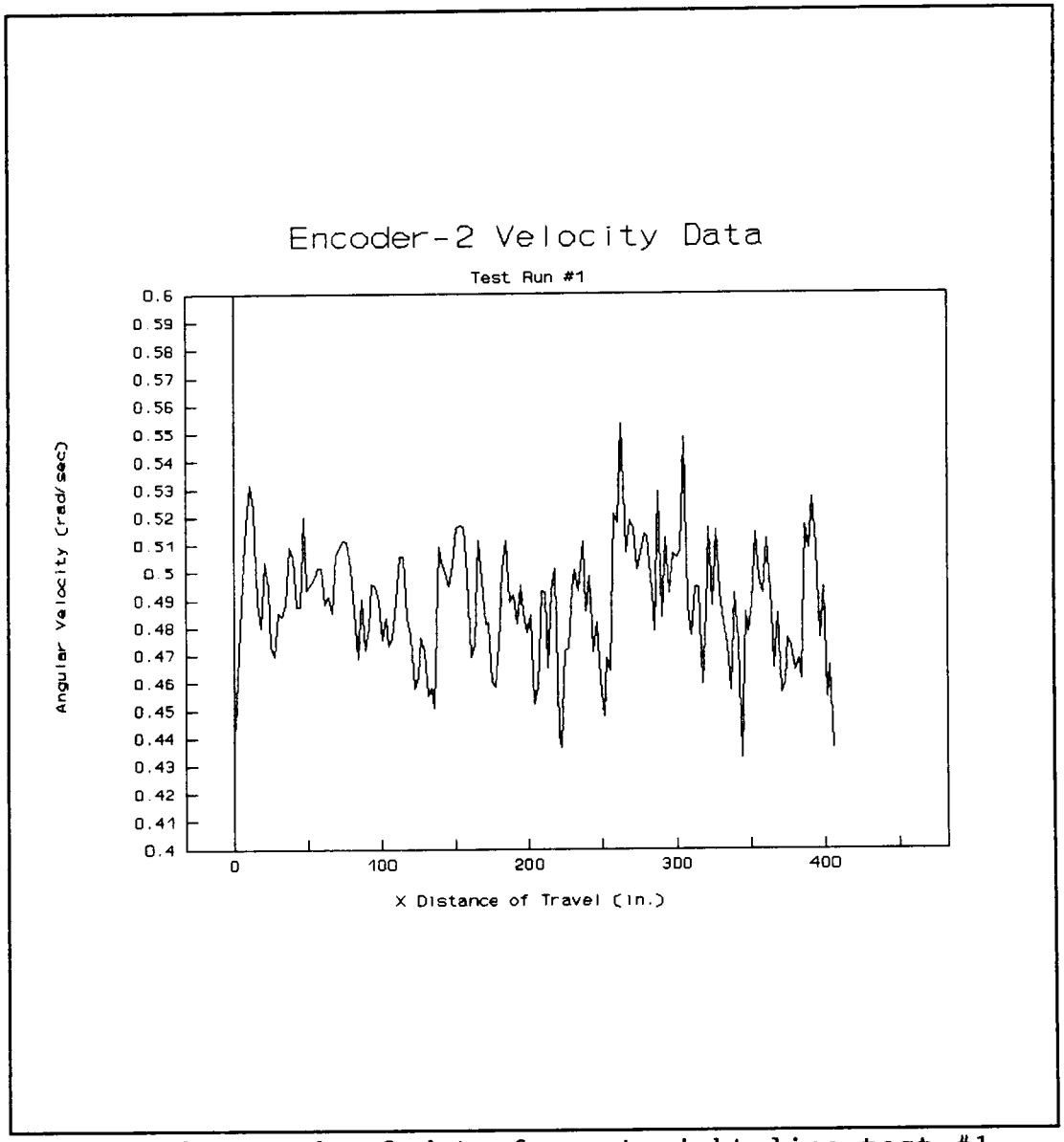

Figure 5.2: Encoder-2 data from straight line test #1

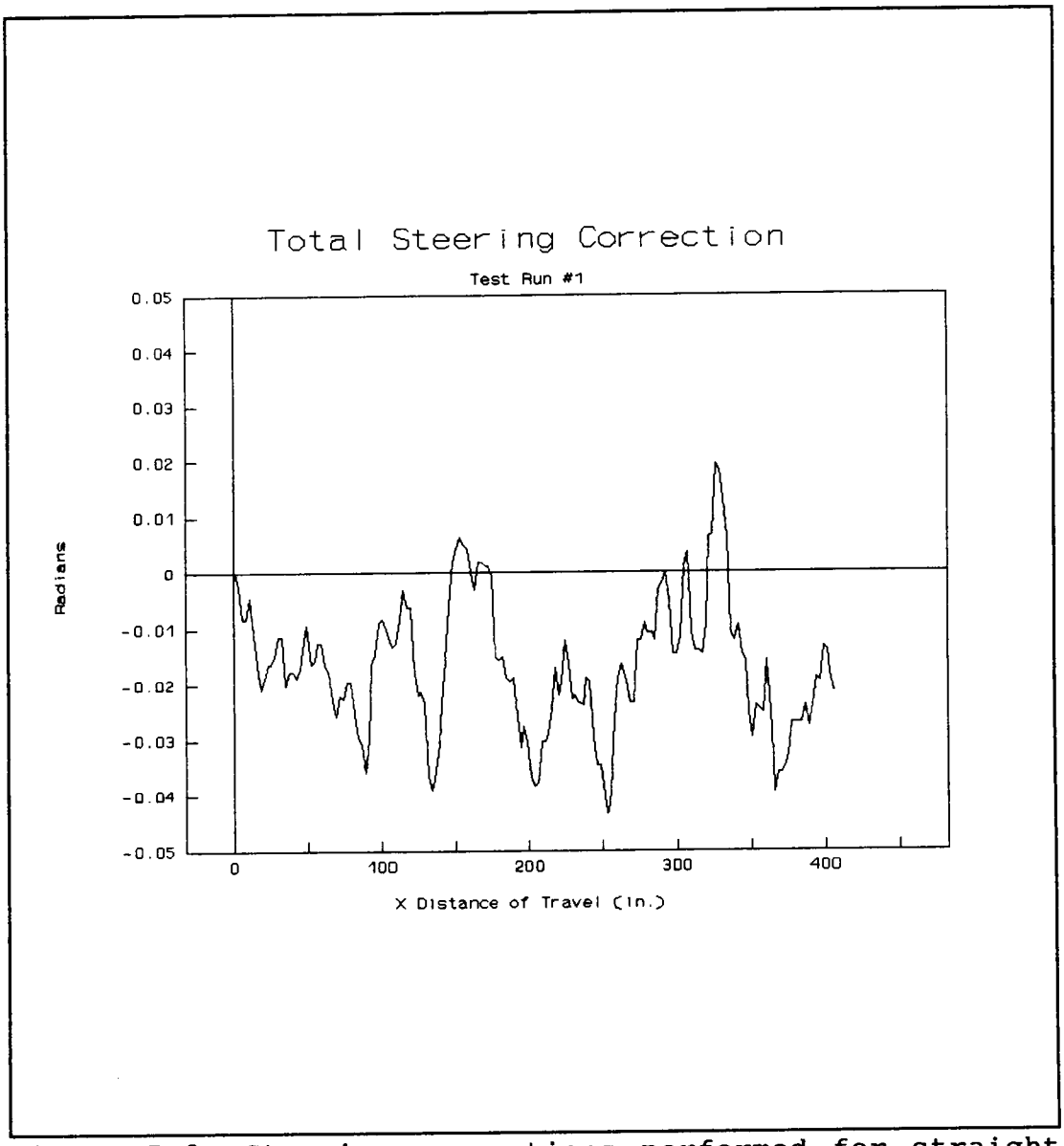

Figure 5.3: Steering corrections performed for straight line test #1

angle was zero relative to the CGV body. In order to instigate these negative steering corrections, encoder-1 should be greater than encoder-2. The problem with the steering corrections lie in the large percentage differences that randomly occur in the velocity readings of the encoders. It was these large differences which caused the control scheme to make corrections for a CGV heading which was different from the true path direction. The velocity data lead to corrections which caused a deviation of the CGV from its programmed path. The random fluctuations in the velocity data can account for the randomness associated with the path deviations discussed in the CGV path analysis.

5.3 RUNNING AVERAGE

A running average of the encoder velocity data plotted against the X distance of travel along with the instantaneous velocity reading at that instant is shown in Figures 5.4 and 5.5. The running average is the average of all the velocity data collected from the beginning of the test run up to, and including, the current encoder velocity reading. From these plots, the running average shows that the CGV should have been traveling in a straight line. The average of the velocity data from encoder-1 was 0.4842 rad/sec, while the average of the velocity data from encoder-2 was 0.4836 rad/sec. These two velocity averages differ by only 0.12%,

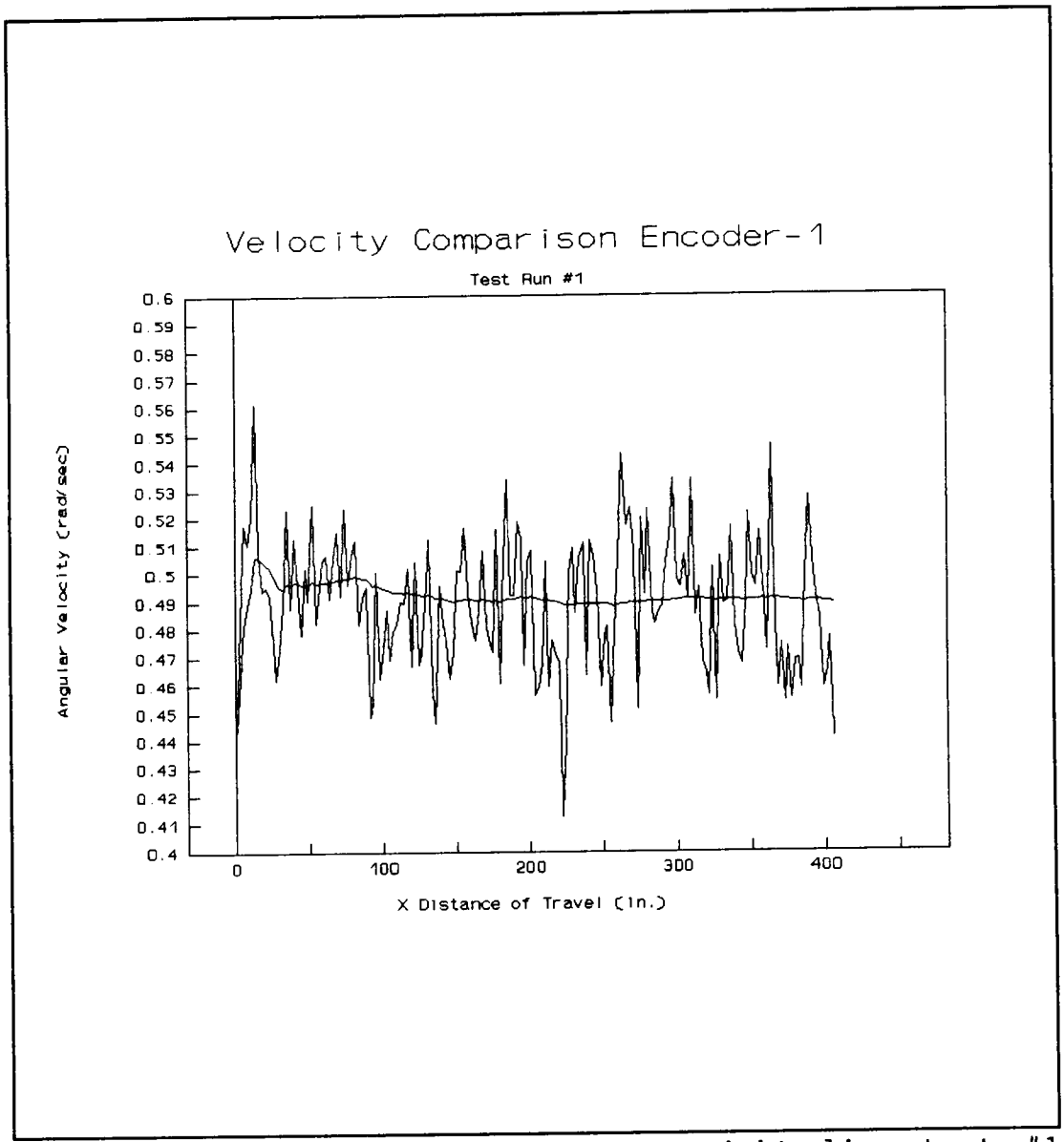

Figure 5.4: Encoder-1 data from straight line test #1 plotted with its running average

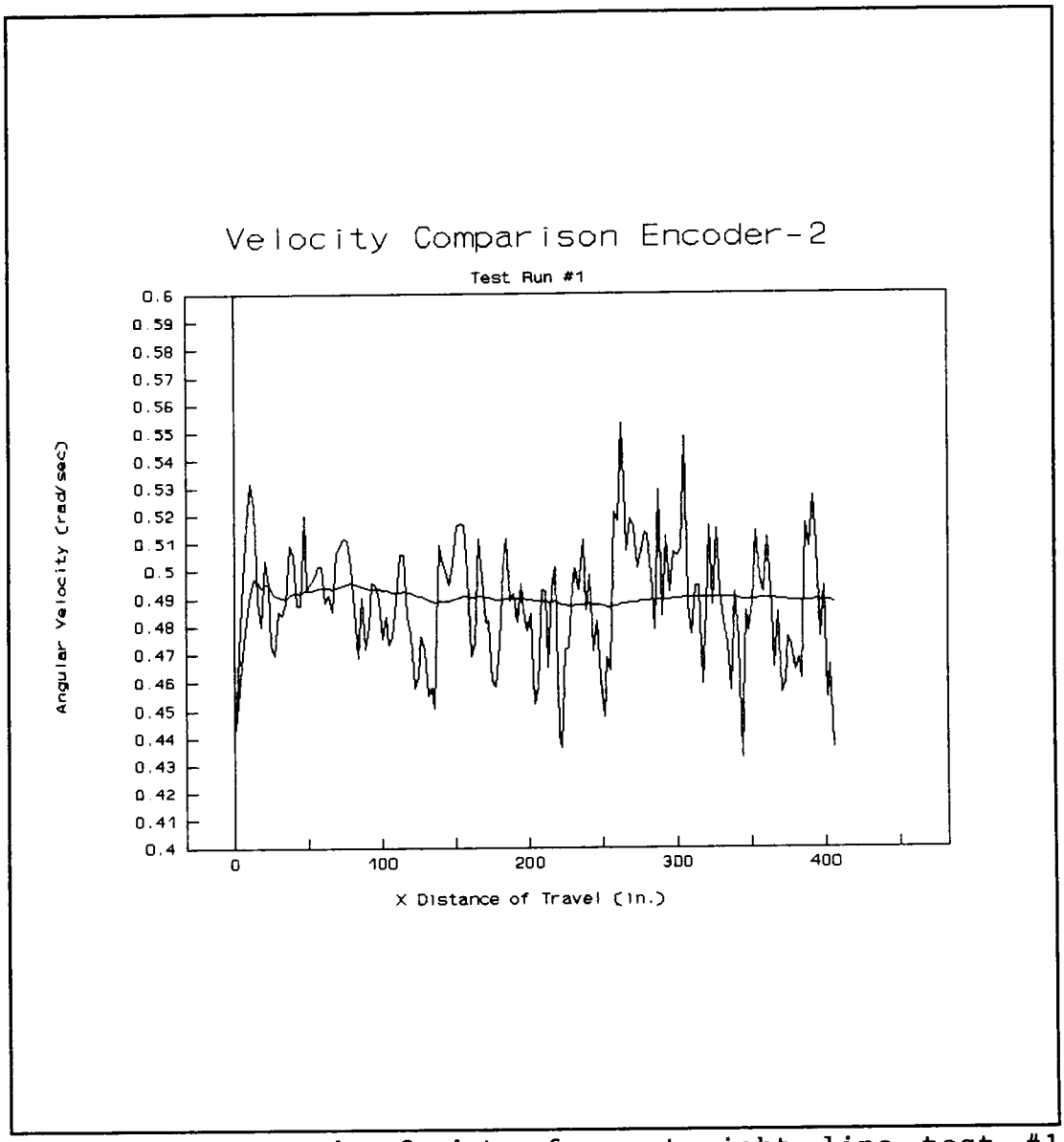

Figure 5.5: Encoder-2 data from straight line test #1 plotted with its running average

indicating that the encoder readings were virtually the same throughout the testing. The random increase (or decrease) in a velocity reading was responsible for "confusing" the computer and resulted in improper path corrections. The characteristics shown in Figures 5.4 and 5.5 are applicable to all of the CGV test run results.

5.4 CONSTANT STEERING ANGLE

Figures 5.6 and 5.7 show the results of the constant steering angle tests which were performed with the CGV. The steering angle of the CGV was fixed to a constant value and no steering corrections were allowed to take place. By fixing the steering angle to a constant value the velocity data received from the encoders should have constant values. The steering angle was set to -0.044 radians in Figure 5.6, and in Figure 5.7 the steering angle was 0.026 radians. In the collection of the velocity data in this test the frequency counter was set on the frequency ratio mode. This allows the frequency counter to read the frequency output of both encoders simultaneously and send the information to the laptop computer in terms of a ratio F_2/F_1, where F_1 and F_2 are the frequency output of encoder-1 and encoder-2, respectively. With the steering angle set to -0.044 radians (Figure 5.6), the encoder ratios should be greater than unity. With a constant negative steering angle, encoder-2 would be further away from the center of

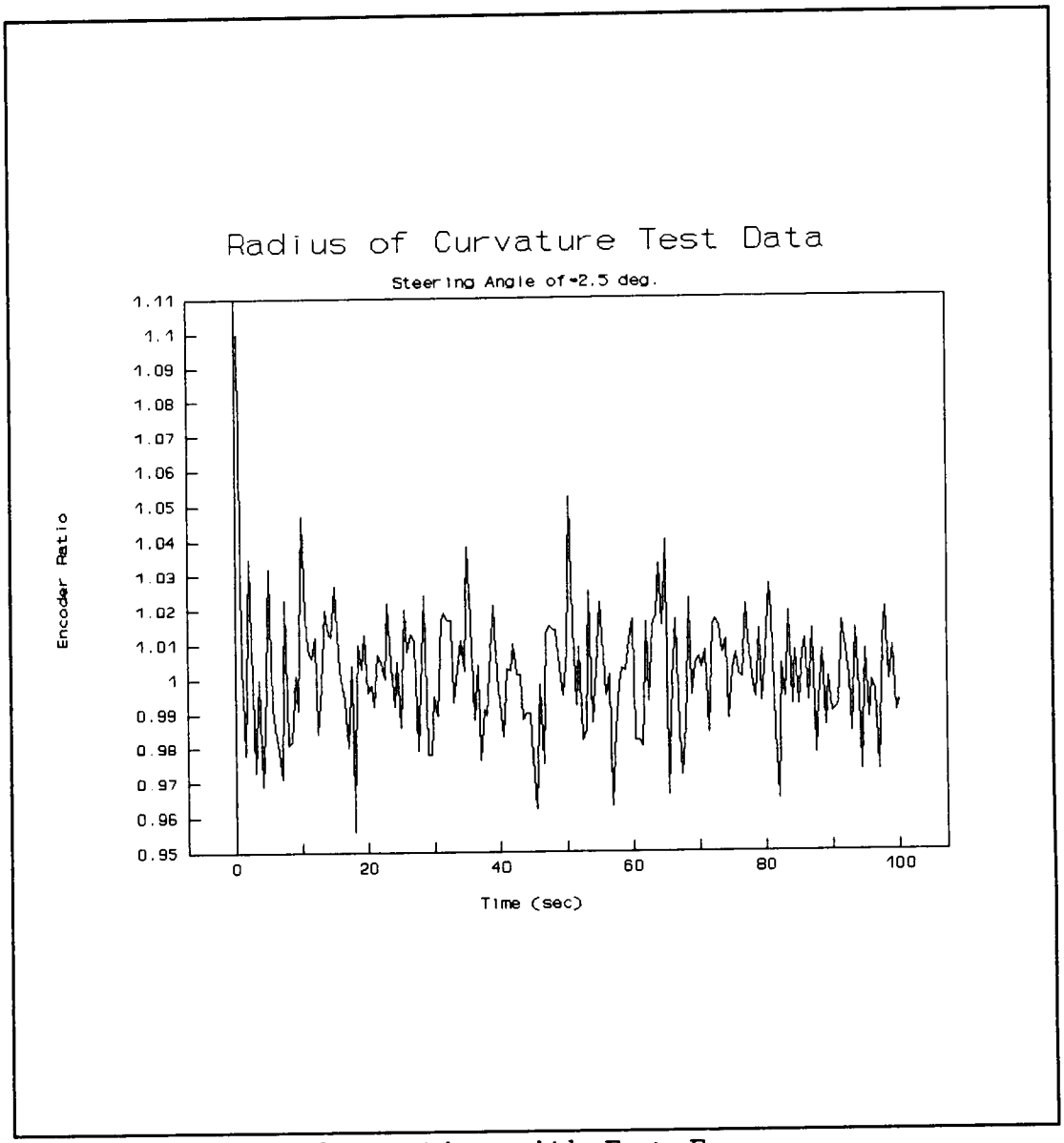

Figure 5.6: Encoder ratios with $F_2 > F_1$

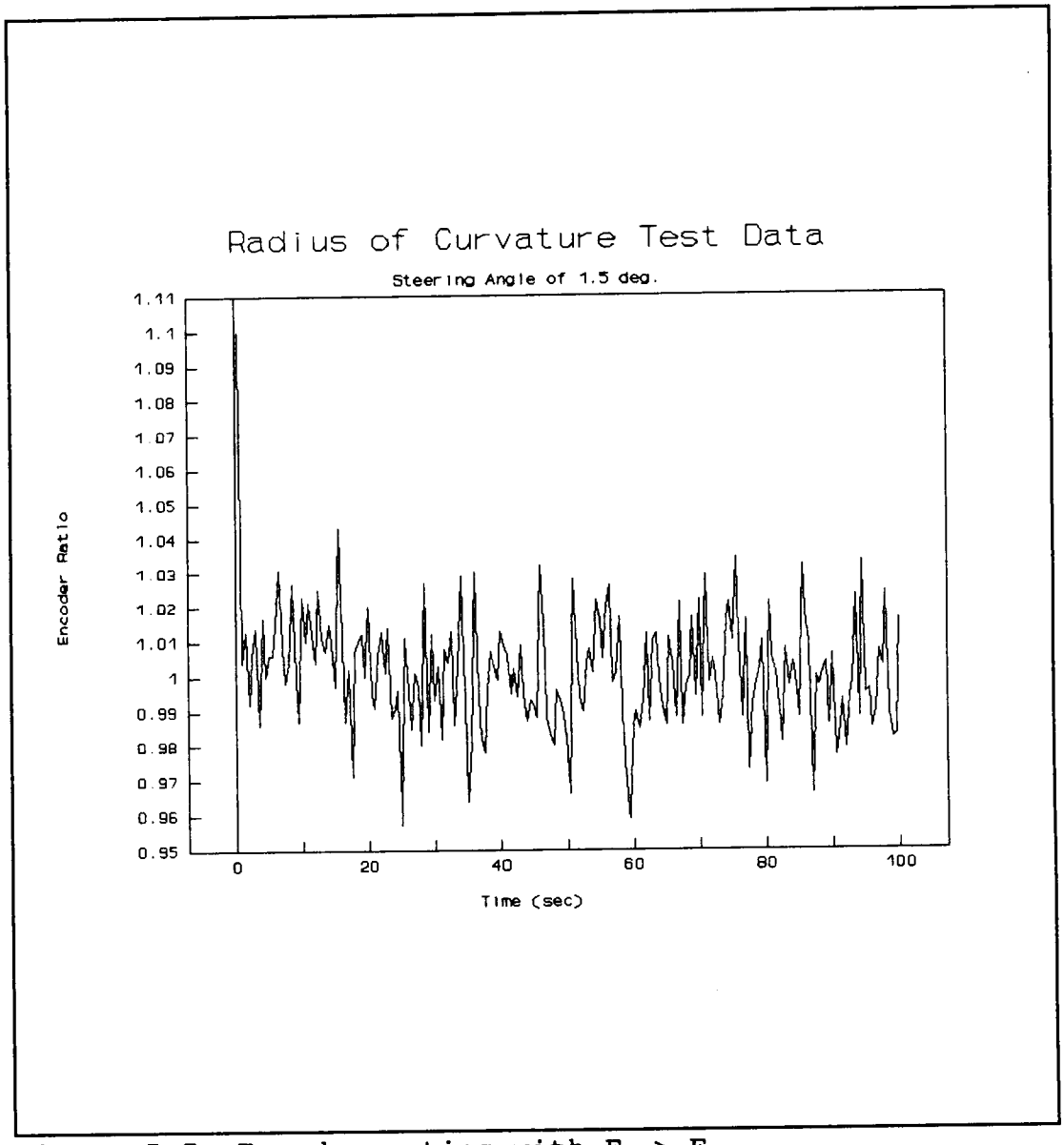

Figure 5.7: Encoder ratios with $F_1 > F_2$

rotation than encoder-1. Thus, with a constant rate of rotation, the velocity readings from encoder-2 must be greater than those of encoder-1 (see Appendix B). In Figure 5.7, with a steering angle of 0.026 radians, the encoder ratios should be less than unity. From the two encoder ratio plots the velocity readings were not constant, with the readings of two successive points differing, at times, by 10%. The randomness in the encoder ratio plots shows that the error that was introduced to the correction scheme was due only to the velocity data received from the encoders.

5.5 RADIUS OF CURVATURE TESTS

Another test conducted to prove the inaccuracy of the velocity readings involved using the total amount of steering the CGV had undergone to calculate the radius of curvature for the CGV. The total amount of steering was found by summing the individual steering corrections performed from the beginning of the test run up to the point of interest. The total amount of steering performed was measured relative to the CGV body. Initially, the angle between the CGV body and the drive wheel was 0 radians. If the absolute value of the total amount of steering is greater than zero, the CGV would travel in a curved path. At any moment the CGV would be rotating about an instantaneous center. The distance from this instantaneous center to the point where the steering

corrections are implemented is the radius of curvature. This analysis was based on data collected from the first test run. The needed information are the angular velocities of the tracking wheels (as given by the encoders) and the total amount of steering performed up to that point. These values were chosen at random from the collected data, see Appendix E. The angular velocities were ω_1=0.5159 rad/sec and ω_2=0.4583 rad/sec. The total amount of steering performed was -0.0154 radians (note: from the negative value of the steering, ω_2 should be greater). Using the collected velocity data, the radius of curvature was calculated to be 205 inches, with the total steering for this radius of curvature calculated to be -0.154 radians. However, the actual amount of steering performed was recorded as -0.0154 radians, which gives a radius of curvature of 2,045 inches. The radius of curvature values differ by 90%. At another location in the collected data from the first test run, angular velocities of ω_1=0.4126 rad/sec and ω_2=0.4362 rad/sec were recorded with the total amount of steering being -0.0199 radians. The radius of curvature calculated from the two angular velocities was 436 inches, giving the total steering angle calculated to be -0.0723 radians. The radius of curvature calculated from the actual steering change (-0.0199 radians) was 1,583 inches - a percentage difference of 72%. From these analyses it is evident that the velocity data from the encoders gave a false picture of the CGV's actual performance.

5.6 BELT SLIP TEST

Tests were conducted to determine if either the timing belts on the steering mechanism were slipping, or if the stepper motor was missing steps during the test runs. These tests would give information which would further isolate the CGV's control problems. This test was conducted by summing the total amount the stepper motor had stepped each correction (taking each corrections directional sign into account). The final value of the number of steps the stepper motor should be from the zero position was printed to the computer screen. The stepper motor was then incremented the corresponding number of steps (in the opposite direction).

Ten test runs were performed and it was determined that the timing belts were not slipping and that the stepper motor was not missing steps as it incremented.

CHAPTER 6

DISCUSSION OF CONTROL SCHEME PERFORMANCE

The accuracy of the control scheme was entirely dependent upon the velocity data received from the encoders. Observations of the control scheme and its performance during simulation and actual testing show that it possesses the three characteristics that all control schemes should have: stability, accuracy, and speed. The developed control scheme has proven to be robust in that it has the capability of dealing with fluctuating velocities (assuming they are correct). The only signs of instability in the control scheme were those induced by varying the maximum correction angle to locate the limits of the CGV's steering stability. None of the test runs performed by the CGV showed signs of instability.

In each simulation test of the control scheme for a straight line path, the CGV never deviated from the desired path by more than ± 0.1 inch. These simulations were performed with simulated random velocities and with velocity data from actual test runs. The accuracy of the CGV control scheme was considered extremely reasonable.

The average time increment between each steering correction of the CGV was approximately 1.9 seconds, where slightly more than 1 second of this period was used to gather the encoder velocity data (gate time and switching). Each

steering correction was performed by the CGV in less than 0.3 seconds implying that the other 0.6 seconds was due to the computer processing time. This period (1.9 seconds) should be reduced to help improve the accuracy of the integration scheme. The time needed to perform the steering correction (0.3 seconds) may not be reducible unless parts of the CGV are redesigned.

CHAPTER 7

RECOMMENDATIONS

Since one of the apparent causes of the CGV's control problem is the velocity data received from the encoders, this area of the vehicle system poses the greatest need for improvement. From tests outlined in Appendix C it was found that the percent difference in the encoder readings is reduced by turning the encoders at higher angular velocities. A test apparatus should be built in which tests can be conducted to determine if the encoders are rotating at too low an angular velocity. If the tests confirm this hypothesis, then a re-design of the CGV's swingarm/tracking wheel/encoder system would be needed.

As discussed in chapter six the control scheme used to determine the correction angle proved to be accurate, fast, and stable. The CGV as a guidance device should be studied further. In the testing of this vehicle design, the only known fallacy was in the false velocity data output by the encoders. It may be that using the encoders in this type of design scheme is a poor choice. Of the three areas in which the CGV depends on for its proper guidance control the only failure is in the velocity data. The other two areas being the integration scheme and the determination of the correction angle.

Although tests were not conducted to prove this point it may be that this guidance vehicle can only be operated on smooth surfaces. Whereas a surface with many bumps or obstacles could hinder the frequency output of the encoders. The major weakness in this guidance device is the failure of the CGV to be able to pickup any axial motion it may move in, if it is accidently hit from the side.

Further study should be given to the initial alignment of the CGV. This area when the tests were conducted had the most room for guess work, since the alignment was based on the authors judgement. Perhaps investigating the need for a three point alignment could prove to be beneficial. Where the three point alignment considers the positioning of the front and rear portions of the CGV, and the initial steering angle.

BIBLIOGRAPHY

BIBLIOGRAPHY

R. H. Hollier, "Automated Guided Vehicles: Proceedings of an Executive Briefing, November 1986," IFS Publications 1986.

R. H. Hollier, "Automated Guided Vehicle Systems," IFS Publications, Bedford, UK, 1987.

Thomas Muller, Automated Guided Vehicles, IFS; Berlin: Springer 1987.

B. B. Hundy, "Proceedings of the 3rd European Conference on Automated Manufacturing May 1985," IFS Publications 1985.

International Conference on Automation in Warehousing, "Proceedings of the 6th International Conference on Automation in Warehousing October 1985," Bedford, IFS Publications 1985.

Takashi Kenjo, Stepping Motors and their Microprocessor Controls, Oxford University Press, New York, 1986.

Ernest O. Doeblin, System Modeling and Response: Theoretical and Experimental Approaches, John Wiley & Sons, New York 1980.

D. T. Greenwood, Principles of Dynamics, Prentice-Hall, Englewood Cliffs, NJ, 1965.

APPENDICES

APPENDIX A

PROGRAM LISTING

```
REM*************************************************************
                        CGV COMPUTER CODE
                           written by
                         David Turner
REM*************************************************************
CLS
REM*************************************************************
REM the frequency counter is reset at the beginning of the
    CGV operation and the communication line between the
    laptop computer and the frequency counter is opened
REM
    OUT &H378, 128
    OPEN "COM2:9600,E,7,1,CS,DS" FOR RANDOM AS #1
REM
REM*************************************************************
REM
REM  Setting the initial parameters:
REM  tht, the current steer angle of the drive wheel wrt the
     horizontal
REM  dx, the distance that is looked ahead to the future
     point
REM  xt and yt, the current x and y positions of the front
     point of the CGV
REM  L, the length from the front point of the car to the
     rear point
REM  UT, the x distance from the front point of the car to
     the rear point
REM  VT, the y distance from the front point of the car to
     the rear point
REM  K1, K2, and K3 are the control gains used in the
     correction angle
REM
REM*************************************************************
10    pi = 4 * ATN(1):
      PRINT "INITIAL SLOPE OF THE VEHICLE WITH RESPECT TO
             THE HORIZONTAL ": INPUT tht
20    dx = 2.5: xt = 0: yt = 0
30    L = 31.5: ut = 31.5: VT = 0
40    k1 = 1: k2 = 1: k3 = 1
REM*************************************************************
CLS
50 FOR tt = 1 TO 500: NEXT tt
60 A = TIMER: OUT &H378, 144
70 FOR j = 1 TO 200
80 IF INKEY$ = CHR$(27) THEN 6000
REM*************************************************************
REM the encoder signals (W1,W2) are read into the computer
    via the serial port
REM*************************************************************
90  OUT &H378, 148
100 GOSUB 4000
110 B$ = ""
```

```
120 IF LOC(1) = 0 THEN 120
130 A$ = INPUT$(LOC(1), #1)
140 B$ = B$ + A$
150 CR = INSTR(B$, CHR$(13))
160 IF CR = 0 THEN 120
170 A$ = LEFT$(B$, CR - 1)
REM **************************
180 W1 = (pi / 9525) * VAL(A$)
REM **************************
190 OUT &H378, 16
200 FOR i = 1 TO 10: NEXT i
210 OUT &H378, 152
220 GOSUB 4000
230 2010 B$ = ""
240 IF LOC(1) = 0 THEN 240
250 A$ = INPUT$(LOC(1), #1)
260 B$ = B$ + A$
270 CR = INSTR(B$, CHR$(13))
280 IF CR = 0 THEN 240
290 A$ = LEFT$(B$, CR - 1)
REM **************************
300 W2 = (pi / 9525) * VAL(A$)
REM **************************
310 OUT &H378, 16
REM************************************************************
REM the first encoder readings are set equal to each other
    due to the initial acceleration of the car
REM************************************************************
320 IF j = 1 THEN W1 = W2
REM************************************************************
REM sd is the linear velocity of the CGV's front point
REM
REM thd is the yaw rate of the CGV
REM************************************************************
330 sd = 1.296 * (W1 + W2): thd = 1.296 * (W1 - W2) / 12.125
REM************************************************************
REM dt is the elapsed time for one cycle of the program and
    the integration step size
REM************************************************************
340 dt = TIMER - A: A = TIMER: PRINT "TIME    "; dt
REM************************************************************
REM th is the angle the car has rotated in dt seconds
REM
REM th is then added to the previous heading of the drive
    wheel
REM
REM tht is the current heading of the CGV drive wheel
REM
REM cs and sn are the cosine and sine of the drive wheel
    heading
REM************************************************************
```

```
350 th = thd * dt: tht = tht + th: cs = COS(tht): sn =
    SIN(tht)
REM*********************************************************
REM the x and y distances traveled in dt seconds is found
REM
REM alp is the yaw of the vehicle body wrt the horizontal,
    it is updated by
REM the addition of the yaw from each velocity reading
REM
REM the total x and y distance traveled (xt,yt) is updated
REM
REM the rear point location of the car (xr,yr) is updated
REM*********************************************************
360 x = sd * cs * dt: y = sd * sn * dt
370 alp = alp + th
380 xt = xt + x: yt = yt + y
390 xr = xt - 31.5 * COS(alp): yr = yt - 31.5 * SIN(alp)
REM
REM*********************************************************
REM start of the correction scheme for a straight line path
REM*********************************************************
REM
REM dy is the y difference in the current and future
    location of the CGV
REM
REM slp is the slope of the desired path
REM
REM dth is the difference in the desired heading and the
    present heading of the CGV
REM
REM rth is the angular correction needed to keep the car on
    path
REM*********************************************************
REM
REM lines 400 and 410 are all that need to be changed to
    alter the CGV path
REM dy = f(xt + dx) - f(xt)
REM slp = f(xt + dx)' - f(xt)'
REM
REM*********************************************************
REM straight line path
REM*********************************************************
400 dy = -yt
410 slp = 0
420 dth = slp - alp
430 rth = k1 * dth - k2 * dx * sn + k3 * dy * cs
REM*********************************************************
REM str is the amount the drive wheel is to be incremented
REM it is a combination of the correction angle and the
    current heading of the CGV drive wheel, it is multiplied
    by .2 to keep the maximum angle of correction to a lower
    limit (this is for stability)
```

```
REM*************************************************************
440 str = (rth - tht - alp) * .2
REM*************************************************************
REM setting the maximum correction angle to 0.025 rad (1.4
    deg)
REM
REM st is the number of steps of the stepping motor
    corresponding to the correction angle
REM
REM SGN takes into account the sign of the correction angle
REM
REM int is used to give a whole number value to the steps
REM
REM thc is set equal to the steering correction increment
REM*************************************************************
450 IF ABS(str) > .025 THEN thc = .025 * SGN(str): GOTO 182
460 thc = str
470 IF thc > 0 THEN st = INT(thc * 5000 / pi): GOTO 490
480 st = INT((-1) * thc * 5000 / pi): GOTO 500
490 FOR i = 1 TO st: OUT &H378, 19: OUT &H378, 18: NEXT i:
    GOTO 510
500 FOR i = 1 TO st: OUT &H378, 17: OUT &H378, 16: NEXT i
REM*************************************************************
REM sta is the actual rotation of the drive wheel found from
    the step count
REM
REM tht is updated with the correction angle
REM*************************************************************
510 sta = SGN(thc) * st * pi / 5000
520 tht = tht + sta
REM*************************************************************
REM*************************************************************
530 NEXT j
6000 OUT &H378, 0
CLOSE
END
REM*************************************************************
REM subroutine used to empty the communications buffer
REM*************************************************************
4000 IF LOC(1) = 0 THEN 4030
4010 ON ERROR GOTO 4040
4020 F$ = INPUT$(LOC(1), #1)
4030 ON ERROR GOTO 0: RETURN
4040 RESUME 4000
```

APPENDIX B

VELOCITY DERIVATIONS

VELOCITY DERIVATIONS

The CGV is a rigid body system translating and rotating on a plane surface. Three coordinates are used to describe the position of the CGV, X, Y, θ, and ω. X and Y are used to describe the linear progression of the CGV with time. θ, describes the yaw of the CGV as a function of time and is measured relative to the X-axis. ω describes the angular velocities of the two tracking wheels. Figure B.1 shows a diagram of the front drive system of the CGV. The drive system in this figure is composed of the two tracking wheels (wheel one and wheel two), and an "imaginary axle" (steer axle) passing between the tracking wheels. The steer axle is perpendicular to the tracking wheels. The center point of the front drive wheel is represented by point C. This center point, C, is the point about which the steering of the CGV occurs. The distance from C to either of the tracking wheels is represented by l. $S^{\cdot}$ is the absolute linear velocity of the CGV. Its direction is always perpendicular to the steer axle passing through the two tracking wheels. The yaw rate of the CGV, $\theta^{\cdot}$, is shown in the Figure B.1 as rotating in the negative direction (clockwise) about the vertical Z-axis. R is the radius of curvature of the CGV. The radius of curvature starts at the center point C, and passes through the tracking wheel to the origin O', of the translating Cartesian coordinate system. Point O' is the instant center of the CGV.

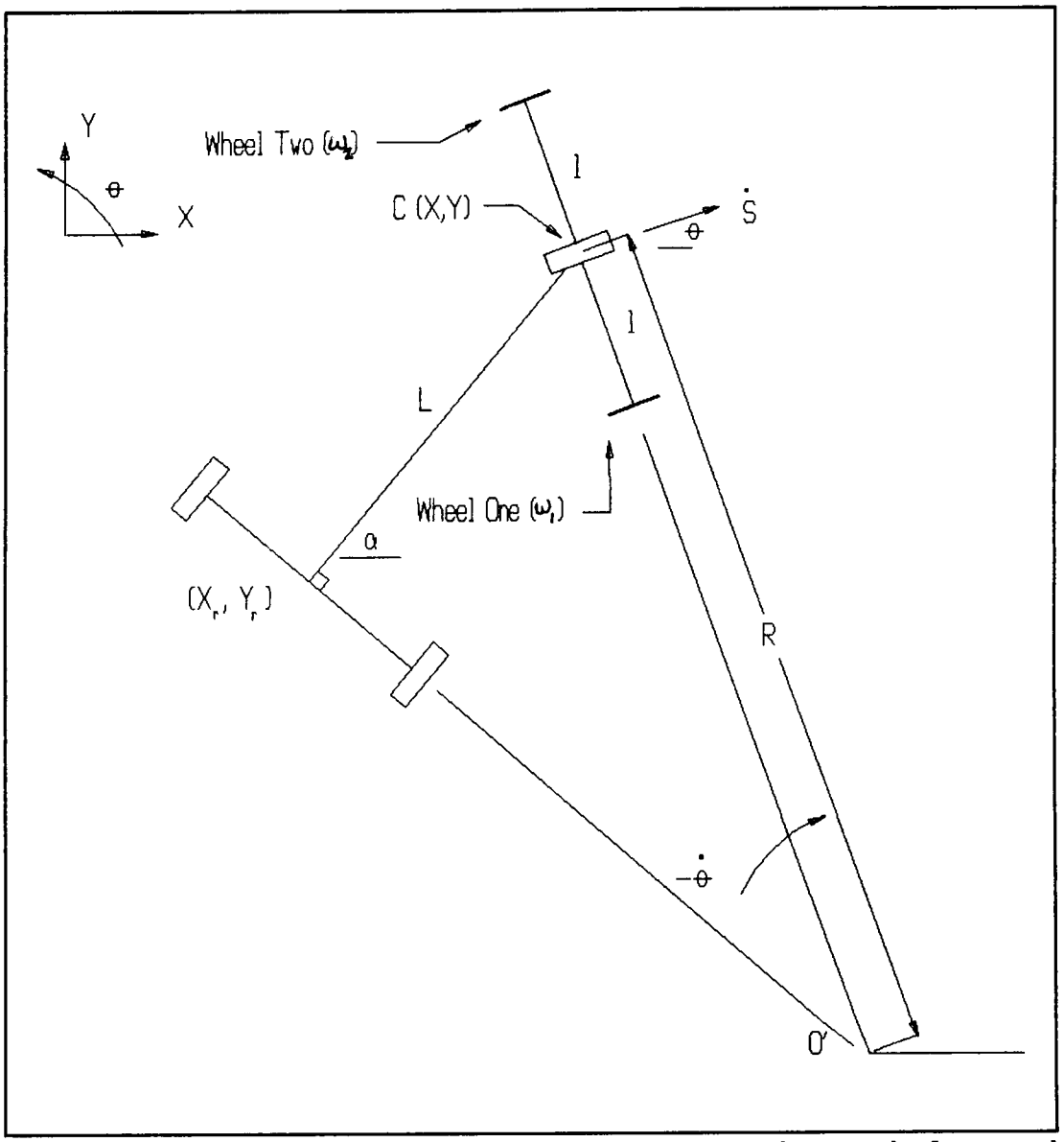

Figure B.1: Wheelbase of the CGV showing the symbols used in the velocity derivations

Each tracking wheel is assumed to be rolling without slipping on the XY plane. The linear velocity of tracking wheel two can be expressed as

$$\vec{V}_2=\vec{V}_{O'}+\vec{V}_{2/O'} \tag{B.1}$$

where

$$\vec{V}_2=r\omega_2\cos(\Theta)\,\vec{i}+r\omega_2\sin(\Theta)\,\vec{j} \tag{B.2}$$

$$\vec{V}_{O'}=0 \tag{B.3}$$

$$\vec{V}_{2/O'}=\dot{\theta}\vec{k}\times(R+l)\vec{r} \tag{B.4}$$

$\times$-*is-the-cross-product*

$$=\dot{\theta}\vec{k}\times[-(R+l)\sin(\Theta)\,\vec{i}+(R+l)\cos(\Theta)\,\vec{j}] \tag{B.5}$$

$$=-\dot{\theta}(R+l)\cos(\theta)\,\vec{i}-\dot{\theta}(R+l)\sin(\theta)\,\vec{j} \tag{B.6}$$

substituting equations (B.2), (B.3), and (B.6) into equation (B.1)

$$r\omega_2\cos(\theta)\,\vec{i}+r\omega_2\sin(\theta)\,\vec{j}=-\dot{\theta}(R+l)\cos(\theta)\,\vec{i}-\dot{\theta}(R+l)\sin(\theta)\,\vec{j}$$

combining like terms gives the result,

$$r\omega_2 = -\dot{\theta}(R+l) \tag{B.7}$$

The linear velocity of tracking wheel one is expressed as

$$\vec{V}_1 = \vec{V}_{O'} + \vec{V}_{1/O'} \tag{B.8}$$

where

$$\vec{V}_1 = r\omega_1 \cos(\theta)\,\vec{i} + r\omega_1 \sin(\theta)\,\vec{j} \tag{B.9}$$

$$\vec{V}_{O'} = 0 \tag{B.10}$$

$$\vec{V}_{1/O'} = \dot{\theta}\vec{k} \times (R-l)\vec{r} \tag{B.11}$$

$$= [\dot{\theta}]\,\vec{k} \times [-(R-l)\sin(\theta)\,\vec{i} + (R-l)\cos(\theta)\,\vec{j}] \tag{B.12}$$

$$= -\dot{\theta}(R-l)\cos(\theta)\,\vec{i} - \dot{\theta}(R-l)\sin(\theta)\,\vec{j} \tag{B.13}$$

substituting equations (B.9), (B.10), and (B.13) into equation (B.11)

$$r\omega_1\cos(\theta)\,\vec{i}+r\omega_1\sin(\theta)\,\vec{j}=-\dot{\theta}(R-l)\cos(\theta)\,\vec{i}-\dot{\theta}(R-l)\sin(\theta)\,\vec{j}$$

combining like terms yields

$$r\omega_1=-\dot{\theta}(R-l) \tag{B.14}$$

from equations (B.7) and (B.14)

$$r\omega_2=-\dot{\theta}R-\dot{\theta}l \tag{B.15}$$

$$r\omega_1=-\dot{\theta}R+\dot{\theta}l \tag{B.16}$$

adding (B.15) and (B.16) gives

$$r(\omega_2+\omega_1)=-2\dot{\theta}R \tag{B.17}$$

the absolute linear velocity of the CGV is

$$\dot{S}=\dot{\theta}\vec{k}\times\vec{R} \tag{B.18}$$

$$=-\dot{\theta}R\cos(\theta)\,\vec{i}-\dot{\theta}R\sin(\theta)\,\vec{j} \tag{B.19}$$

substituting (B.17) into (B.19)

where

$$\dot{S}=\frac{r}{2}(\omega_2+\omega_1)\cos(\theta)\,\vec{i}+\frac{r}{2}(\omega_2+\omega_1)\sin(\theta)\,\vec{j} \qquad (B.20)$$

$$\dot{X}=\frac{r}{2}(\omega_2+\omega_1)\cos(\theta) \qquad (B.21)$$

$$\dot{Y}=\frac{r}{2}(\omega_2+\omega_1)\sin(\theta) \qquad (B.22)$$

subtracting (B.16) from (B.17) gives an expression for the yaw rate of the CGV

$$\dot{\theta}=\frac{r}{2l}(\omega_1-\omega_2) \qquad (B.23)$$

Equations (B.21) and (B.22) which describe the linear velocity of the CGV are nonholonomic constraints. These two equations adhere to the rolling without slipping assumption made earlier. Because (B.21) and (B.22) are nonholonomic they cannot be integrated. However, if the two angular velocities, ω_1 and ω_2, are specified along with the angle of the steer axle, Θ. Then X and Y˙ can be numerically integrated to find the X and Y position of the CGV. The angular velocities are given by the encoders and the yaw is given by integrating $\dot{\Theta}$.

The velocity equations which describe the movement of the rear point of the car are derived in the following manner. The heading of the CGV body can be described as

$$\alpha = ATN\left(\frac{\dot{Y}_r}{\dot{X}_r}\right) = ATN\left(\frac{Y-Y_r}{X-X_r}\right) \qquad (B.24)$$

$$\frac{\dot{Y}_r}{\dot{X}_r} = \frac{Y-Y_r}{X-X_r} \qquad (B.25)$$

$$U = X - X_r \qquad (B.26)$$

$$\dot{U} = \dot{X} - \dot{X}_r \qquad (B.27)$$

$$V = Y - Y_r \qquad (B.28)$$

$$\dot{V} = \dot{Y} - \dot{Y}_r \qquad (B.29)$$

equation (B.25) is manipulated to give the following

$$\frac{\dot{Y}-\dot{Y}_r-\dot{Y}}{\dot{X}-\dot{X}_r-\dot{X}} = \frac{Y-Y_r}{X-X_r} \qquad (B.30)$$

Where (B.30) can be expressed as

$$\frac{\dot{V}-\dot{Y}}{\dot{U}-\dot{X}} = \frac{V}{U} \qquad (B.31)$$

rearranging (B.31) gives

$$\dot{V}U-\dot{Y}U=\dot{U}V-\dot{X}V \tag{B.32}$$

the physical constraint of the CGV is given by

$$U^2+V^2=l^2 \tag{B.33}$$

by use of the chain rule (B.33) becomes

$$2\dot{U}U+2\dot{V}V=0 \tag{B.34}$$

from this exact relationship we obtain

$$\dot{U}=-\dot{V}(\frac{V}{U}) \tag{B.35}$$

Substituting (B.35) into (B.32)

$$\dot{V}U-\dot{Y}U=-\dot{V}\frac{V^2}{U}-\dot{X}V \tag{B.36}$$

Rearranging the terms and using the physical constraint from (B.33)

$$\dot{V}U+\dot{V}\frac{(l^2-U^2)}{U}=\dot{Y}U-\dot{X}V \tag{B.37}$$

the final form of the equations for the X and Y movement of the rear point are

$$\dot{V}=\frac{U^2\dot{Y}-VU\dot{X}}{l^2} \tag{B.38}$$

$$\dot{U}=-\dot{V}\left(\frac{V}{U}\right) \tag{B.39}$$

These velocities are integrated to obtain the rear position of the CGV. The angle α, is given by equation (B.24).

APPENDIX C

HARDWARE TESTS

HARDWARE TESTS

Tests were conducted to try an isolate the source of the CGV's position error. From the computer simulation results it became clear that the problem was in the encoders' velocity data. Each part of the CGV's hardware which had a role in passing the encoder signals from the encoders to the laptop computer were tested. These were the circuit used to perform the switching, the frequency counter, the computer code's input lines, and the encoder themselves.

The circuit used to switch from one encoder reading to the other encoder reading was tested in the following ways. First a known generated signal was allowed to pass through the circuit, without switching, and the frequency output analyzed. Then the same signal was passed through the circuit but in this test switching was allowed to take place.

After the above two tests were completed each encoder was tested independently. The tests conducted on the encoders were the following. First a DC motor was used to rotate the encoders at different angular velocities ranging from 1000 pulse/sec up to 18,000 pulse/sec. Second a pulse count test was performed by rotating each tracking a known number of turns to determine if each encoder was counting pulses correctly. The actual number of pulses the encoder should output was calculated. Next the pulse counts were conducted by pushing the CGV along the test surface (the CGV

was held at a constant steer angle). This test would mirror the conditions in which the velocity data from the encoders was collected as described in chapter four.

The next series of tests involved inputting the encoder signals to an oscilloscope. The oscilloscope would give important information pertaining to the characteristics of each encoders squarewave signal. The amplitude and period of the oscilloscope display could be compared to the amplitude and period of each encoder's input signal. This would give information in regard to the quality of each of the encoder squarewave signals.

The frequency counter was first tested with a signal of known frequency. The generated signal was a 2000 hz squarewave, which was comparable to the signal output by the encoders. The generated signal was input into the circuit at the location where the encoder signals were received. The generated signal replaced the encoders. As in the actual test runs of the CGV the laptop computer was used to obtain the frequency information from the frequency counter. The method of data collection by the laptop computer was not altered. Once the frequency data was collected it was displayed on the laptop computer's screen. The primary objectives of this test were to conclude if a) the frequency counter was being used improperly, b) the encoder signals were being mixed during the switching process, and c) noise was distorting the encoder signals.

It was possible that noise generated by the stepper driver and the DC gear motor were distorting the encoder signals. To test this possibility the stepper driver and the DC motor were on at all times during the testing.

With the generated signal passing the encoder-1 input line, no switching, the frequency displayed by the frequency counter remained constant for over 100 samples. The generated signal was then input through the encoder-2 input line. The displayed frequency did not change.

The second test was designed to test the switching process used to alternate the encoder readings. To conduct this test the same signal was used and input to both encoder lines. This was to simulate the affect of having two active encoders, and allowed switching from one signal to the other. The results of this test were the same as the previous: no change occurred in the displayed frequencies. As before 100 samples were collected. Varying gate times were used with only slight changes in accuracy. Below Tables C.1 and C.2 summarize the results of the tests performed while switching between the two encoder input lines. An average of 100 samples is given along with a percent difference between the maximum and minimum readings.

Table C.1: Frequency output of the generated signal through the encoder-1 input line

Gate (sec)	Average (Hz)	Largest % Difference
0.05	2280.913	0.1030
0.50	2279.759	0.0644
1.50	2280.350	0.0587

Table C.2: Frequency output of the generated signal through the encoder-2 input line

Gate (sec)	Average (Hz)	Largest % Difference
0.05	2280.884	0.1126
0.50	2279.739	0.0889
1.50	2280.377	0.0412

From these tests it was concluded that the frequency counter was being used properly and that the signals were not being mixed by the multiplexor.

The next set of tests used a DC motor to turn each tracking wheel at a velocity near those in actual test runs. This test would give information on how the encoders perform in a static situation. Various gate times were used for this test and the results are shown in the tables which follow.

Table C.3: Frequency output of encoder-1 using a DC motor to turn encoder-1

Gate (sec)	Average (Hz)	Largest % Difference
0.05	1017.564	5.51
0.50	1016.766	3.16
1.50	1013.185	2.85

Table C.4: Frequency output of encoder-2 using a DC motor to turn encoder-2

Gate (sec)	Average (Hz)	Largest % Difference
0.05	1006.857	9.72
0.50	1013.395	2.51
1.50	1016.303	1.75

These results have the same pattern as those shown in Tables C.1 and C.2. The percent difference decreases with increasing gate time. The above results also show a random average between the two encoders.

Tables C.5 and C.6 show the results when the encoder's angular velocity is increased.

Table C.5: Frequency output of encoder-1 using a DC motor to turn encoder-1

Gate (sec)	Average (Hz)	Largest % Difference
0.05	18,086	7.6
0.50	18,200	0.8
1.50	17,989	1.20

Table C.6: Frequency output of encoder-2 using a DC motor to turn encoder-2

Gate (sec)	Average (Hz)	Largest % Difference
0.05	18,305	9.2
0.50	18,236	0.85
1.50	18,219	1.40

From these results it is shown that at higher angular velocities the percent difference in the high and low frequency readings of the encoders is reduced.

The pulse count tests revealed that the encoders were giving consistent pulse counts. When the tracking wheels

were rotated a fixed number of revolutions the encoders always output the correct number of pulses. When the tracking wheels were turned 20 revolutions the encoders output a pulse count of 380,810 pulses, 0.05% from the actual value of 381,000. When the CGV was pushed along the test surface the largest percent difference of any two pulse counts from 20 test runs was 0.47% occurring with encoder-2.

When the encoder signal was input to an oscilloscope it was found that the encoder speed significantly affected the quality of the output squarewave. At low frequencies of approximately 1000 pulse/sec, the period of the squarewave was not steady but would fluctuate along the time scale of the oscilloscope. However at frequencies of 18,000 pulse/sec the quality of the squarewave's period was much improved.

All of the above tests show that at higher angular velocities the encoder output is greatly improved. It was also concluded that noise from the hardware was not interfering with the encoder output.

APPENDIX D

STEERING ARC DERIVATIONS

STEERING ARC DERIVATIONS

The following derivation shows the analysis which was used to account for the arc the drive wheel travels during each steering correction. It was found during testing that this method required too much computer time to be affective. It involved finding the change in the CGV's position due to each increment of the stepper motor during the steering corrections. Figure D.1 shows the CGV orientation used in this derivation, where V_f and V_r are the front and rear point velocities.

The velocity of the front point is given by

$$\vec{V}_f = V_f \cos(\theta)\,\vec{i} + V_f \sin(\theta)\,\vec{j} \qquad (D.1)$$

where the rear point velocity can be expressed as

$$\vec{V}_r = \vec{V}_f + \vec{V}_{r/f} \qquad (D.2)$$

where

$$\vec{V}_{r/f} = \dot{\theta}\vec{k} \times \vec{L} \qquad (D.3)$$

$$\dot{\theta}\vec{k} = \frac{V_f}{R}\vec{k} \qquad (D.4)$$

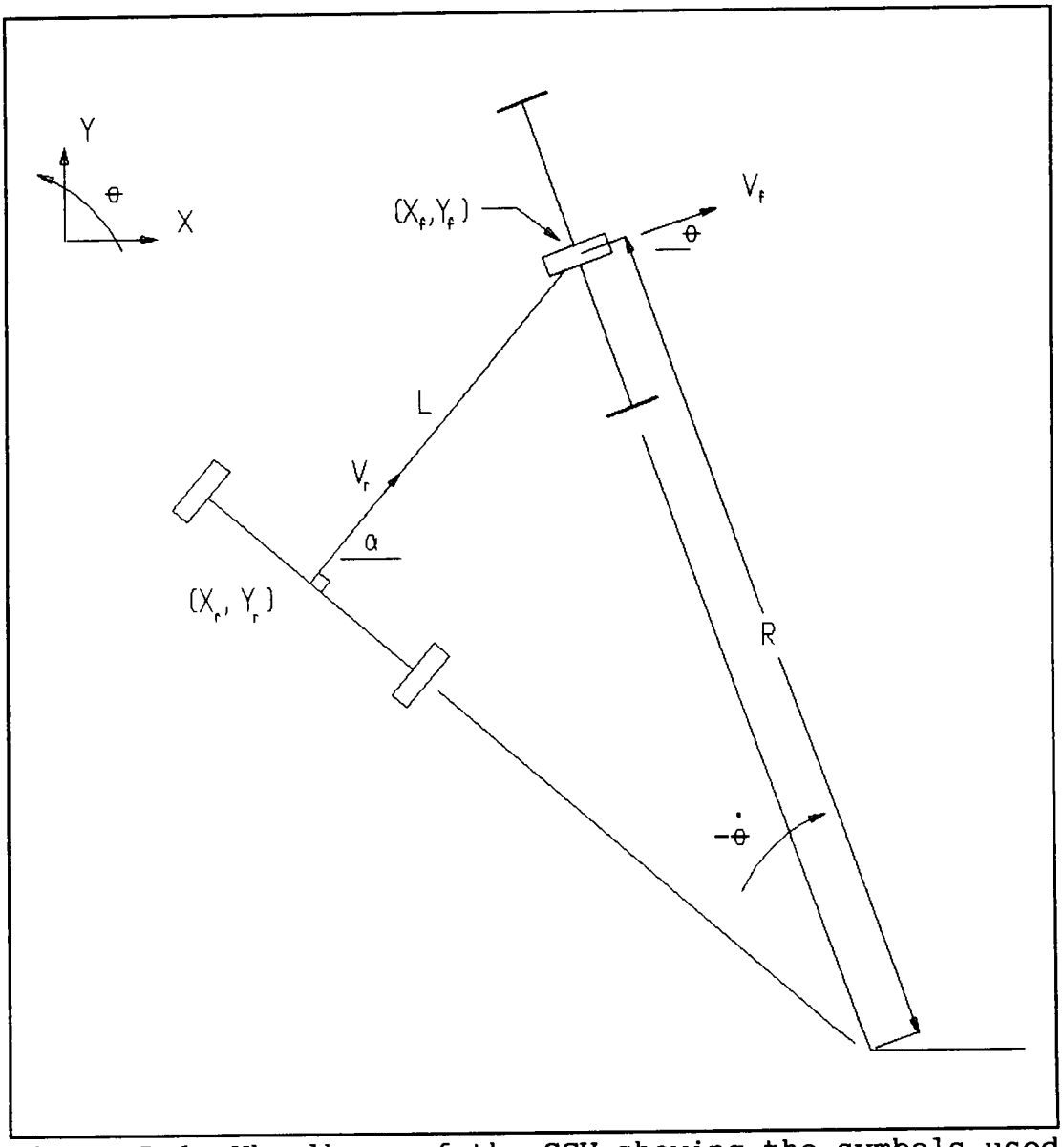

Figure D.1: Wheelbase of the CGV showing the symbols used in the derivations for the steering arc

$$R=\frac{L}{\sin(\theta-\phi)} \tag{D.5}$$

$$\vec{L}=-L\cos(\phi)\,\vec{i}-L\sin(\phi)\,\vec{j} \tag{D.6}$$

from (D.4) and (D.6), equation (D.3) becomes

$$\vec{V}_{r/f}=\frac{V_f}{R}L\sin(\phi)\,\vec{i}-\frac{V_f}{R}L\cos(\phi)\,\vec{j} \tag{D.7}$$

substituting (D.1) and (D.7) into (D.2) gives

$$\vec{V}_r=V_f\cos(\theta)\,\vec{i}+V_f\sin(\theta)\,\vec{j}+\frac{V_f}{R}L\sin(\phi)\,\vec{i}+\frac{V_f}{R}L\cos(\phi)\,\vec{j} \tag{D.8}$$

the change in the front point position from (D.1) is

$$\Delta X_f=V_f\cos(\theta)\,dt \tag{D.9}$$

$$\Delta Y_f=V_f\sin(\theta)\,dt \tag{D.10}$$

the change in the rear point position from (D.8)

$$\Delta X_r=\Delta X_f+\frac{V_f}{R}L\sin(\theta)\,dt \tag{D.11}$$

substituting (D.5)

$$\Delta X_r=\Delta X_f+V_f\sin(\theta)\sin(\phi-\theta)\,dt \tag{D.12}$$

$$\Delta Y_r = \Delta Y_f - \frac{V_f}{R} L\cos(\phi)\, dt \qquad (D.13)$$

$$\Delta Y_r = \Delta Y_f - V_f \cos(\phi)\sin(\phi-\theta)\, dt \qquad (D.14)$$

$$\theta_{new} = \theta_{old} + \Delta\theta_{steer} + \dot{\theta}\, dt \qquad (D.15)$$

$$X_{f_{new}} = X_{f_{old}} + \Delta X_f \qquad (D.16)$$

$$\Delta Y_{f_{new}} = Y_{f_{old}} + \Delta Y_f \qquad (D.17)$$

$$X_{r_{new}} = X_{r_{old}} + \Delta X_r \qquad (D.18)$$

$$Y_{r_{new}} = Y_{r_{old}} + \Delta Y_r \qquad (D.19)$$

$$\phi_{new} = ATN\left(\frac{Y_f - Y_r}{X_f - X_r}\right) \qquad (D.20)$$

APPENDIX E

DATA FROM TEST #1

w1	w2	str.	xt	yt	tht	alp	time
0.4434	0.4434	0.0000	1.3916	0.0000	0.0000	0.0000	1.2109
0.4825	0.4708	-0.0025	3.6261	0.0051	0.0023	0.0023	3.0195
0.5175	0.4966	-0.0057	6.0081	0.0141	0.0038	0.0063	4.8320
0.5105	0.5171	0.0000	8.4946	0.0063	-0.0032	0.0050	6.6992
0.5202	0.5318	0.0038	10.9656	-0.0071	-0.0054	0.0029	8.5117
0.5612	0.5231	-0.0063	13.5072	0.0074	0.0057	0.0101	10.3203
0.5067	0.4893	-0.0057	15.9226	0.0144	0.0029	0.0136	12.1914
0.4937	0.4800	-0.0044	18.3429	0.0146	0.0001	0.0164	14.1094
0.4950	0.5037	0.0019	20.7647	-0.0001	-0.0061	0.0147	15.9805
0.4924	0.4947	0.0025	23.1438	-0.0111	-0.0046	0.0142	17.8398
0.4815	0.4730	0.0000	25.5309	-0.0119	-0.0003	0.0160	19.7695
0.4621	0.4696	0.0013	27.7759	-0.0161	-0.0018	0.0145	21.6289
0.4727	0.4855	0.0038	30.1722	-0.0237	-0.0032	0.0119	23.5586
0.4883	0.4838	0.0000	32.5935	-0.0202	0.0015	0.0123	25.4805
0.5233	0.4884	-0.0088	35.0416	0.0005	0.0084	0.0198	27.3477
0.4876	0.5093	0.0025	37.5245	-0.0115	-0.0048	0.0153	29.2695
0.5126	0.5056	0.0000	39.9885	-0.0137	-0.0009	0.0167	31.1357
0.4953	0.4876	-0.0013	42.3720	-0.0122	0.0006	0.0182	33.0078
0.4791	0.4876	0.0019	44.7138	-0.0181	-0.0025	0.0163	34.8789
0.5019	0.5199	0.0050	47.2536	-0.0291	-0.0043	0.0126	36.7969
0.4904	0.4936	0.0025	49.7044	-0.0290	0.0000	0.0120	38.7188
0.5251	0.4961	-0.0069	52.1756	-0.0084	0.0084	0.0178	40.5859
0.4822	0.4984	0.0006	54.6132	-0.0129	-0.0019	0.0145	42.5039
0.4915	0.5017	0.0031	57.0216	-0.0209	-0.0033	0.0124	44.3750
0.5048	0.5013	0.0000	59.5223	-0.0194	0.0006	0.0131	46.2930

0.5063	0.4884	-0.0038	61.9345	-0.0074	0.0042	0.0167	48.1641
0.4912	0.4911	-0.0013	64.3811	-0.0084	0.0004	0.0167	50.0859
0.5058	0.4854	-0.0050	66.8449	-0.0002	0.0033	0.0209	52.0039
0.5148	0.5064	-0.0031	69.3886	-0.0002	0.0000	0.0226	53.9258
0.4919	0.5086	0.0038	71.8096	-0.0158	-0.0065	0.0193	55.7930
0.5236	0.5111	-0.0006	74.3032	-0.0164	-0.0002	0.0218	57.6523
0.4961	0.5108	0.0031	76.8212	-0.0261	-0.0039	0.0188	59.5820
0.5068	0.5015	0.0000	79.3327	-0.0231	0.0004	0.0199	61.5039
0.5116	0.4861	-0.0057	81.7471	-0.0120	0.0055	0.0249	63.3711
0.4816	0.4686	-0.0044	84.1138	-0.0061	0.0025	0.0276	65.2930
0.4915	0.4704	-0.0013	86.5546	-0.0102	-0.0017	0.0279	67.2109
0.4952	0.4715	-0.0050	88.9626	-0.0056	0.0019	0.0327	69.1328
0.4482	0.4799	0.0063	91.3131	-0.0259	-0.0095	0.0254	71.0039
0.4534	0.4956	0.0132	93.4998	-0.0534	-0.0116	0.0180	72.8633
0.5007	0.4948	0.0019	95.9794	-0.0464	0.0029	0.0192	74.7852
0.4625	0.4897	0.0057	98.3461	-0.0484	-0.0009	0.0136	76.7031
0.4733	0.4752	0.0096	100.7229	-0.0380	0.0044	0.0132	78.6367
0.4871	0.4834	-0.0019	103.0614	-0.0245	0.0057	0.0139	80.4961
0.4689	0.4734	-0.0013	105.3465	-0.0178	0.0030	0.0130	82.3672
0.4796	0.4757	-0.0019	107.7211	-0.0118	0.0025	0.0138	84.2952
0.4815	0.4898	0.0006	110.0766	-0.0142	-0.0010	0.0122	86.1563
0.4898	0.5054	0.0044	112.4900	-0.0229	-0.0035	0.0090	88.0273
0.4892	0.5056	0.0050	114.9629	-0.0299	-0.0025	0.0057	89.9453
0.5018	0.4834	-0.0031	117.4167	-0.0134	0.0063	0.0095	91.8672
0.4670	0.4773	0.0000	119.7639	-0.0199	0.0011	0.0074	93.7852

0.5042	0.4579	-0.0113	122.0969	0.0132	0.0103	0.0166	95.6563
0.4672	0.4618	-0.0044	124.4813	0.0136	0.0002	0.0177	97.6367
0.4707	0.4763	0.0006	126.7729	0.0013	-0.0054	0.0166	99.5039
0.4895	0.4716	-0.0019	129.1035	-0.0015	-0.0012	0.0202	101.3750
0.5123	0.4550	-0.0132	131.5077	0.0174	0.0087	0.0319	103.2930
0.4577	0.4579	-0.0025	133.7383	0.0091	-0.0045	0.0319	105.2148
0.4480	0.4507	0.0019	136.0306	-0.0089	-0.0080	0.0309	107.1445
0.4955	0.5093	0.0063	138.5334	-0.0314	-0.0090	0.0281	109.0664
0.4856	0.5038	0.0075	140.9926	-0.0472	-0.0064	0.0244	110.9844
0.4758	0.4996	0.0075	143.4221	-0.0563	-0.0038	0.0195	112.9063
0.4622	0.4948	0.0094	145.8156	-0.0634	-0.0030	0.0128	114.8359
0.4720	0.5023	0.0082	148.2374	-0.0627	0.0003	0.0065	116.7539
0.5012	0.5158	0.0025	150.7807	-0.0469	0.0054	0.0035	118.6836
0.5004	0.5168	0.0019	153.2321	-0.0375	0.0047	0.0003	120.5430
0.5163	0.5162	-0.0013	155.8142	-0.0205	0.0066	0.0003	122.4727
0.4934	0.4990	-0.0006	158.2862	-0.0102	0.0042	-0.0009	124.3945
0.4819	0.4693	-0.0044	160.5929	0.0038	0.0061	0.0017	126.2656
0.4759	0.4734	-0.0031	162.9529	0.0089	0.0022	0.0022	128.1836
0.4872	0.5113	0.0050	165.4399	-0.0058	-0.0059	-0.0023	130.1055
0.5081	0.4970	0.0000	167.9383	-0.0023	0.0014	-0.0005	132.0234
0.4808	0.4811	-0.0006	170.2709	0.0008	0.0013	-0.0005	133.8945
0.4763	0.4818	0.0000	172.6526	-0.0002	-0.0004	-0.0017	135.3125
0.4716	0.4603	-0.0019	174.9123	0.0040	0.0018	0.0006	137.6836
0.5159	0.4583	-0.0145	177.3387	0.0327	0.0118	0.0124	139.6055
0.4604	0.4735	-0.0006	179.6601	0.0203	-0.0053	0.0098	141.5234

0.5052	0.5005	0.0006	182.0939	0.0081	-0.0050	0.0107	143.3906
0.5338	0.5113	-0.0038	134.6969	0.0087	0.0002	0.0153	145.3125
0.4920	0.4888	-0.0006	137.0706	0.0019	-0.0029	0.0160	147.1797
0.4918	0.4917	0.0006	189.4555	-0.0065	-0.0035	0.0160	149.0508
0.5187	0.4815	-0.0069	191.8809	0.0046	0.0046	0.0234	150.9219
0.5123	0.4951	-0.0057	194.3849	0.0076	0.0012	0.0269	152.8398
0.4669	0.4855	0.0038	196.7668	-0.0123	-0.0083	0.0231	154.7695
0.5044	0.4783	-0.0025	199.1346	-0.0108	0.0006	0.0293	156.6289
0.5081	0.4843	-0.0063	201.5360	-0.0039	0.0029	0.0330	158.4961
0.4563	0.4520	-0.0019	203.7985	-0.0096	-0.0025	0.0339	160.4180
0.4589	0.4584	0.0006	206.0786	-0.0194	-0.0043	0.0340	162.3359
0.4676	0.4930	0.0075	208.4713	-0.0407	-0.0089	0.0288	164.2578
0.5041	0.4927	0.0000	210.9640	-0.0383	0.0010	0.0311	166.1875
0.4594	0.4649	0.0013	213.1914	-0.0385	-0.0001	0.0301	168.0469
0.4757	0.4935	0.0044	215.6151	-0.0446	-0.0025	0.0264	169.9766
0.4710	0.5009	0.0075	217.9572	-0.0541	-0.0041	0.0205	171.8359
0.4620	0.4409	-0.0050	220.2163	-0.0336	0.0091	0.0260	173.7539
0.4126	0.4362	0.0025	222.3304	-0.0354	-0.0008	0.0212	175.6758
0.4383	0.4713	0.0075	224.5362	-0.0462	-0.0049	0.0146	177.5469
0.5003	0.4725	-0.0044	226.3804	-0.0271	0.0082	0.0201	179.4063
0.5090	0.4938	-0.0063	229.3122	-0.0103	0.0068	0.0231	181.2773
0.4860	0.5006	0.0006	231.7045	-0.0163	-0.0024	0.0202	183.1484
0.5055	0.4928	-0.0013	234.1252	-0.0144	0.0008	0.0228	185.0195
0.5110	0.5110	-0.0006	236.6708	-0.0136	-0.0005	0.0223	186.9414
0.4632	0.4859	0.0050	238.9675	-0.0236	-0.0056	0.0182	188.3086

0.5120	0.4983	-0.0006	241.4839	-0.0230	0.0022	0.0211 190.7305
0.5063	0.4711	-0.0101	243.7133	-0.0016	0.0088	0.0283 172.6484
0.4933	0.4815	-0.0050	246.3561	0.0014	0.0012	0.0307 194.5820
0.4592	0.4609	0.0000	248.6431	-0.0082	-0.0042	0.0304 196.5000
0.4771	0.4475	-0.0057	250.3853	-0.0043	0.0017	0.0363 198.3711
0.4810	0.4688	-0.0031	253.1835	-0.0073	-0.0015	0.0337 200.2383
0.4462	0.4642	0.0038	255.3911	-0.0257	-0.0082	0.0351 202.1094
0.4790	0.5207	0.0132	257.8757	-0.0582	-0.0130	0.0266 204.0273
0.5059	0.5176	0.0075	260.5024	-0.0642	-0.0023	0.0241 206.0078
0.5429	0.5531	0.0025	263.2321	-0.0556	0.0032	0.0220 207.9297
0.5170	0.5070	-0.0031	265.7930	-0.0358	0.0077	0.0241 209.8594
0.5234	0.5186	-0.0038	268.3041	-0.0219	0.0055	0.0250 211.7138
0.5079	0.5154	0.0000	270.8632	-0.0212	0.0002	0.0235 213.6484
0.4511	0.5007	0.0113	273.2337	-0.0448	-0.0099	0.0133 215.5703
0.5199	0.5069	0.0000	275.7860	-0.0345	0.0040	0.0160 217.4883
0.4925	0.5138	0.0031	278.2261	-0.0351	-0.0002	0.0117 219.3594
0.5229	0.5128	-0.0019	280.7324	-0.0227	0.0049	0.0137 221.2266
0.4854	0.4930	0.0000	283.1717	-0.0135	0.0017	0.0124 223.1484
0.4918	0.4784	-0.0013	285.5000	-0.0130	0.0024	0.0131 225.0195
0.4862	0.5288	0.0088	288.0229	-0.0322	-0.0076	0.0043 226.9375
0.4879	0.4836	0.0013	290.4522	-0.0271	0.0021	0.0052 228.8672
0.5036	0.5125	0.0019	292.9831	-0.0234	0.0015	0.0034 230.7891
0.5127	0.4921	-0.0050	295.4144	-0.0051	0.0075	0.0075 232.6563
0.5337	0.5067	-0.0094	297.9371	0.0147	0.0079	0.0129 234.5273
0.4974	0.5051	0.0000	300.4289	0.0069	-0.0031	0.0113 236.4453

0.4950	0.5074	0.0031	302.8441	-0.0067	-0.0056	0.0098 239.3047
0.5063	0.5484	0.0126	305.4656	-0.0337	-0.0111	0.0002 240.2227
0.4905	0.4871	0.0025	307.9154	-0.0304	0.0023	0.0009 242.1563
0.5338	0.4766	-0.0145	310.4266	0.0109	0.0164	0.0125 244.0742
0.4849	0.4943	-0.0031	312.9399	0.0108	-0.0000	0.0106 246.0547
0.4946	0.4943	0.0000	315.3229	0.0034	-0.0031	0.0107 247.9141
0.4681	0.4591	-0.0006	317.5713	0.0005	-0.0013	0.0125 249.7852
0.4640	0.4857	0.0050	319.8598	-0.0138	-0.0062	0.0082 251.6445
0.4563	0.5160	0.0157	322.2123	-0.0447	-0.0131	-0.0037 253.5117
0.5020	0.4874	0.0006	324.6765	-0.0309	0.0056	-0.0007 255.4336
0.4544	0.5149	0.0126	327.1006	-0.0460	-0.0062	-0.0132 257.3633
0.5061	0.4919	-0.0013	329.5813	-0.0231	0.0092	-0.0102 259.2813
0.4887	0.4815	-0.0050	331.9978	-0.0002	0.0095	-0.0088 261.2031
0.4896	0.4738	-0.0069	334.3925	0.0182	0.0077	-0.0055 263.1211
0.5166	0.4571	-0.0170	336.8275	0.0500	0.0131	0.0068 265.0508
0.4814	0.4919	-0.0013	339.3159	0.0347	-0.0061	0.0046 267.0234
0.4712	0.4746	0.0025	341.6811	0.0156	-0.0081	0.0038 268.9531
0.4673	0.4326	-0.0050	343.8498	0.0184	0.0013	0.0107 270.8125
0.4896	0.4853	-0.0013	346.2881	0.0115	-0.0028	0.0116 272.7422
0.5217	0.4783	-0.0094	348.7788	0.0235	0.0048	0.0205 274.6641
0.4992	0.4680	-0.0044	351.2327	0.0179	-0.0023	0.0229 276.5820
0.4952	0.5139	0.0057	353.7460	-0.0085	-0.0105	0.0190 278.5039
0.5147	0.4968	-0.0006	356.2757	-0.0115	-0.0012	0.0227 280.4336
0.4961	0.4922	-0.0006	358.7324	-0.0139	-0.0010	0.0235 282.3516
0.4724	0.5118	0.0094	361.1039	-0.0364	-0.0095	0.0157 284.2109

0.5462	0.4857	-0.0125	363.7522	-0.0026	0.0128	0.0285	286.1914
0.4962	0.4651	-0.0113	366.1466	0.0132	0.0066	0.0349	288.1133
0.4592	0.4846	0.0039	368.5691	-0.0112	-0.0101	0.0295	290.0938
0.4743	0.4560	0.0000	370.8202	-0.0173	-0.0027	0.0331	291.9609
0.4537	0.4598	0.0013	373.0355	-0.0259	-0.0039	0.0319	293.8339
0.4732	0.4758	0.0019	375.3367	-0.0332	-0.0032	0.0314	295.7031
0.4548	0.4729	0.0057	377.5863	-0.0443	-0.0049	0.0277	297.5742
0.4688	0.4640	0.0000	379.9095	-0.0493	0.0017	0.0287	299.4961
0.4692	0.4682	0.0000	382.1778	-0.0360	0.0019	0.0289	301.3633
0.4584	0.4610	0.0000	384.3934	-0.0329	0.0014	0.0294	303.2227
0.4987	0.5167	0.0031	386.8558	-0.0383	-0.0022	0.0248	305.0938
0.5275	0.5082	-0.0038	389.4303	-0.0257	0.0049	0.0288	307.0117
0.5047	0.5265	0.0038	392.0092	-0.0344	-0.0034	0.0243	308.9414
0.4923	0.5088	0.0050	394.4215	-0.0414	-0.0029	0.0210	310.8008
0.4836	0.4758	-0.0006	396.7479	-0.0327	0.0037	0.0226	312.6719
0.4586	0.4941	0.0063	399.0592	-0.0420	-0.0040	0.0155	314.5430
0.4651	0.4542	-0.0006	401.3479	-0.0317	0.0045	0.0177	316.4648
0.4769	0.4660	-0.0044	403.5916	-0.0174	0.0061	0.0199	318.3828
0.4408	0.4365	-0.0031	405.8856	-0.0117	0.0026	0.0208	320.3125

APPENDIX F

FREQUENCY COUNTER SPECIFICATIONS

8.0 SPECIFICATIONS

8.1 GENERAL INFORMATION

Programmable Functions:	Frequency, Period, Time Interval A to B, Frequency Ratio B/A, Totalize
Scale Factor:	-99999 to 999999 with a choice of six decimal point positions (9.9.9.9.9.9.), multiply or divide
Offset:	-99999 to 999999 with a choice of six decimal point positions (9.9.9.9.9.9.)

8.2 INPUT CHARACTERISTICS

Max Frequencies (A and B inputs square wave, 0 to +5 V):	SA and SB on F positions: 7 MHz (min)
	SA and SB on M positions: 200 kHz (typ)
	SA and SB on S positions: 3 kHz (typ)
Trigger Slopes (A and B):	Positive or Negative, programmable
Input Threshold:	All TTL and CMOS compatible except spare flip-flop inputs, which are:
	5 V, CMOS compatible (Low = less than 0.9 V, High = more than 3.5 V)
Input Impedance:	A, B and External Gate inputs: 20 k pull-up
	$\overline{\text{HOLD}}$ input: 100 k pull-up (typ) $\overline{\text{RESET}}$ input: 10 k pull-up
Max Input Voltage : (A and B)	SA and SB on F positions: -0.5 and +5.5 V
	SA and SB on M or S positions: -20 and +25 V
Max Input Voltage : (all other inputs)	-0.5 and 5.5 V

8.3 DISPLAY

Type:	7-segment, orange LED with red lens
Digit Height:	14.2 mm (.56 in)
Symbols:	-.8.8.8.8.8. and 8.8.8.8.8.8.
Decimal Point:	Six positions; programmable Fixed or auto-ranging
Leading Zeros:	Blank or displayed; programmable
Overflow Indication:	Display in exponential format to 9.99 E9
Update Time:	Averaging time + (10-40 milliseconds) + communication time
Brightness:	100%, 50%, 25%; programmable
Displayed Value:	(Measurement · Scale Factor) + Offset
Indicator Lights:	GATE LED; Low and High alarm LEDs
Capacity:	
decimal format	-99999 or 999999
exponential format	-9.9×10^{9} or 9.99×10^{9}

8.4 OUTPUT CHARACTERISTICS

Lo, Hi and Go Alarm Outputs:	Open-collectors, active low, 150 mA at 1 V
Digit 6:	High level = 3.5 V at 100 μA Low level = 0.4 V at 1.6 mA Frequency = 400 Hz ±.1%

8.5 TIME BASE

Internal Clock Reference:	11.059 MHz
Stability:	±50 ppm over 0-60°C range
Fine-Calibration method:	Programmable calibration value
Calibration accuracy at 25°C:	±2 ppm

8.6 COMMUNICATION

RS-232 OUT, IN and RTS:		RS-232 C compatible with transmit handshake line (RTS)
		Levels: ±5 V
Transmitted data:		Alarm + 6 digits + decimal point + CR (9 characters)
	or	Alarm + 6 digits + d.p. + space + units of measurement + CR (12 characters)
Baud rate:		1200 or 9600 baud, programmable
Received data:		Complete setup parameters, no handshake
0-20 mA ASCII out:		Open collector (data the same as RS-232 OUT)
Bit serial BCD (Internal connection to parallel BCD board):		32 bits; display and alarm data. When enabled, takes about 10 milliseconds to be transmitted.

8.7 FREQUENCY/PERIOD FUNCTION

Frequency range:	10^{-6} Hz to 7 MHz (140 nsec to 36 days)
Nominal Gate Time (NGT):	00.00 to 99.99 seconds
Averaging Time (Actual Gate Time):	(NGT + 2.7 ms) or Ext. Gate Time + time to complete the last period
Max Ext. Gate Time:	$\frac{6 \times 10^{10}}{F_A}$ or 36 days, whichever is less
Units-of-Measurement (Scale Factor = 1):	Frequency: hertz Period: milliseconds
Accuracy at 25°C: (Auto-range SA on F Position)	±1 LSD ±2 ppm of input

Calculation time:	Scale Factor is a multiplier; 20-35 ms Scale Factor is a divider; 30-45 ms
Max speed (gate time minimum) (Parallel BCD disabled, RTS false):	20-40 readings/second

8.8 TIME INTERVAL

Interval range, A to B:	400 ns to 36 days
Trigger error (A - B):	SA and SB on F positions: +30 ±70 ns SA and SB on M positions: +30 ±250 ns SA and SB on S positions: ±9 μs
Accuracy, NGT = 00.00:	±1 LSD ± trigger error ± TI (Time Base Error)
Accuracy, NGT ≠ 00.00:	± 1 LSD ± trigger error ± $\frac{\text{(T.B. Error) TI}}{\sqrt{N}}$, where N is number of averaged intervals
Number of averaged intervals:	$N = \frac{\text{(Averaging Time) X Frequency}}{2}$
Nominal Gate Time (NGT):	00.00 to 99.99 seconds, in .01 sec steps
Averaging time:	NGT = 00.00: .1 ms + time to complete the last interval NGT ≠ 00.00: NGT + 2.5 ms + time to complete the last interval
Averaging method:	Every other Time Interval
Unit of Measurement: (Scale Factor = 1)	milliseconds

8.9 FREQUENCY RATIO, $\frac{B}{A}$

B input frequency range:	0.007 Hz to 7 MHz
A input frequency range:	$F_B > 5$ kHz: 10^{-6} Hz to 7 MHz $F_B < 5$ kHz: $\frac{1}{F_A} + \frac{1}{F_B} < 160$ sec
Nominal Gate Time (NGT):	00.00 to 99.99 seconds, in .01 sec steps

Averaging time:	(NGT + 2.5 ms) or Ext. Gate Time + time to complete the last period of A and B
Resolution: (SA and SB on F positions)	$F_B > 5$ kHz: $\frac{1}{(\text{Averaging Time}) \times F_B}$
	$F_B < 5$ kHz: $\frac{1}{5000 \times (\text{Averaging Time})}$
Max External Gate Time:	$\frac{6 \times 10^{10}}{F_A}$ or $\frac{3.5 \times 10^{13}}{F_B}$, whichever is less

8.10 TOTALIZE

Count direction:	Up or Down (determined by sign of scale factor)
LSD: (Auto-range, Scale Factor=1)	1 count of the input
Internal count capacity:	(60,000,000,000) 6×10^{10} counts
AC power failure provisions:	Display value stored in nonvolatile memory and restored with power

8.11 POWER

+5 V output:	Regulated, 50 mA max in nontotalize modes (1) (reduced by upper-board option)
V+ output:	Unregulated, 6-9 V, 50 mA max in nontotalize modes (1) (reduced by upper-board option and current drawn from the +5 V output)
AC voltage (standard):	115 or 230 V ac ±10% 47 to 400 Hz
Power consumption:	3 W, typical
Battery backup: (connected to V+ with a diode)	6-12 V, 50 mA (typ), without upper-board option

NOTE: In totalize mode, 20 mA can be drawn from +5 V or V+ when display brightness is normal or dim (CnFG 2 = XXXXX1). Up to 50 mA can be drawn if the BLANK ENABLE input is tied to GND. This prevents a power failure detection.

APPENDIX G

OPTICAL ISOLATOR CHIP SPECIFICATIONS

PRELIMINARY SPECIFICATION

NEC ELECTRON DEVICE

PS2502-1,-2,-3,-4

DARLINGTON MULTI PHOTOCOUPLER

FEATURES

1. High isolation voltage
2. Small package
3. High CTR ---- CTR: 200 % MIN

APPLICATION

1. Sequence controler
2. Telephone sets, Telephone exchanges

ABSOLUTE MAXIMUM RATINGS (Ta=25°C)

	SYMBOL	PS2502-1	PS2502-2,3,4,	UNIT
DIODE				
Reverse Voltage	V_R	6	6	V
Forward Current	I_F	80	80	mA
Peak Forward Current*	$I_{F(peak)}$	1	1	A
Power Dissipation	P_D	150	120	mW/unit
TRANSISTOR				
Collector to Emitter Voltage	V_{CEO}	40	40	V
Emitter to Collector Voltage	V_{ECO}	7	7	V
Collector Current	I_C	200	160	mA
Power Dissipation	P_C	150	120	mW/unit
Isolation Voltage**	BV	5000	5000	Vrms
Operating Temperature	Topt	-55 to +100	-55 to +100	°C
Storage Temperature	Tstg	-55 to +150	-55 to +100	°C
Lead Temperature (10 sec)		260	260	°C

* PW=100 μs ,Duty Ratio=1%

** Condition
AC voltage for 1 minute at Ta=25°C,RH=60%
between input and output.

APPENDIX H

MULTIPLEXOR CHIP SPECIFICATIONS

National Semiconductor

CD4066BM/CD4066BC Quad Bilateral Switch

General Description

The CD4066BM/CD4066BC is a quad bilateral switch intended for the transmission or multiplexing of analog or digital signals. It is pin-for-pin compatible with CD4016BM/CD4016BC, but has a much lower "ON" resistance, and "ON" resistance is relatively constant over the input-signal range.

Features

- Wide supply voltage range — 3 V to 15 V
- High noise immunity — 0.45 V_{DD} (typ.)
- Wide range of digital and analog switching — ±7.5 V_{PEAK}
- "ON" resistance for 15 V operation — 80 Ω
- Matched "ON" resistance over 15 V signal input — ΔR_{ON} = 5 Ω (typ.)
- "ON" resistance flat over peak-to-peak signal range
- High "ON"/"OFF" output voltage ratio — 65 dB (typ.) @ f_{is} = 10 kHz, R_L = 10 kΩ
- High degree linearity — 0.1% distortion (typ.) @ f_{is} = 1 kHz, V_{is} = 5 V_{p-p}, $V_{DD} - V_{SS}$ = 10 V, R_L = 10 kΩ
- Extremely low "OFF" switch leakage — 0.1 nA (typ.) @ $V_{DD} - V_{SS}$ = 10 V, T_A = 25°C
- Extremely high control input impedance — 10^{12} Ω (typ.)
- Low crosstalk between switches — −50 dB (typ.) @ f_{is} = 0.9 MHz, R_L = 1 kΩ
- Frequency response, switch "ON" — 40 MHz (typ.)

Applications

- Analog signal switching/multiplexing
  - Signal gating
  - Squelch control
  - Chopper
  - Modulator/Demodulator
  - Commutating switch
- Digital signal switching/multiplexing
- CMOS logic implementation
- Analog-to-digital/digital-to-analog conversion
- Digital control of frequency, impedance, phase, and analog-signal-gain

Schematic and Connection Diagrams

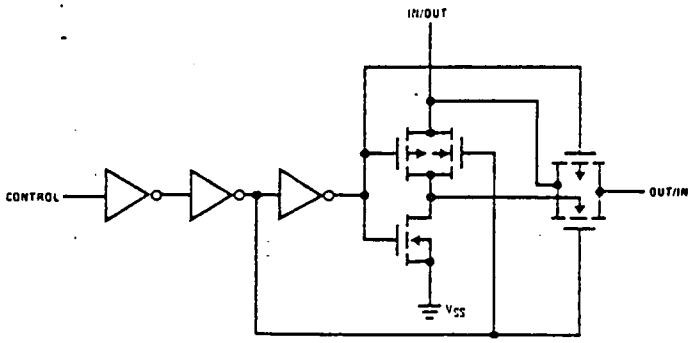

Dual-In-Line Package

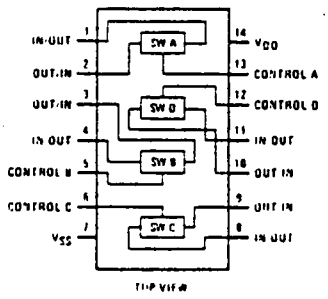

APPENDIX I

ENCODER SPECIFICATIONS

M23 Modular Incremental Encoders

PMI PMI PMI

OUTPUT CIRCUITS

Table 1

Model	Voltage	IC	Type	Output Structure	Max. Rating
Squarewave	5V	SN7404	TTL	Standard & Complementary	−16 ma
		SN7406	TTL	Open Collector	−40 ma @ 30 V
Squarewave	12 & 15 V	MM74C04	CMOS	Standard & Complementary	10 ma @ 15 V
Amplified Sinewave	±15V 5V (Index)	TL082 LM393	Op AMP Comp.	Bi-Polar TTL Compatible	17 ma 16 ma

OUTPUT TABLE

Function	Wire Color
Output A	White
Output B	Blue
Index	Green
V+	Red
Common	Black
*Output $\overline{A}$	Brown/White
*Output $\overline{B}$	Blue/White
*$\overline{\text{Index}}$	Orange
** + 15V	Red/White
** − 15V	Black/White

* Additional outputs for complementary models

** Split supply for amplified sinewave

INPUT POWER

Table 2

Model	Voltage	Current
All Squarewave	5, 12 or 15V ± 5%	100 ma max.
Amplified Sinewave	± 15V ± 5% 5V ± 5%	20 ma max. 100 ma max.

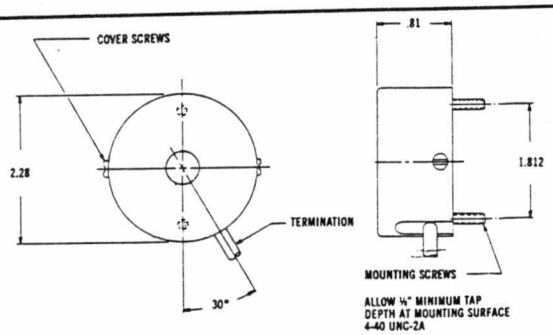

Mounting Interface Requirements
(for 500 lines typical)

Shaft axial endplay	0.001 in
Shaft runout	0.002 in TIR
Shaft squareness to mounting face	0.002 in
Shaft extension	0.7 in min.

NOTES:

1. Other track densities are available on a special order basis.
2. For information on non-standard output formats such as X2, X4, line drivers and direction sensing, please contact PMI Motors. We will be happy to discuss your application requirements.

Model Numbers For M23 Modular Encoders

M23-0500-ABI - 5 - S - P -.3750

Model

Cycles per Revolution

50	256	600	1500
60	300	720	1800
100	360	800	2000
180	400	900	2048
200	500	1000	2500
250	508	1024	3540
254	512	1200	

Number of Outputs
AB - Channels A & B
ABI - A, B and Index

Voltage
5 = 5V
12 = 12V
15 = 15V (±15V if sinewave)

Output Circuit
S = Standard squarewave
O = Open collector (5V model only)
C = Complementary
**A = Amplified sinewave

Leads
P - Pigtails, 18" min.
C - Shielded cable 18" min.

***Hub Size** $^{+.0002}_{-.0000}$
.2500 (1/4 in.)
.3750 (3/8 in.)
.5000 (1/2 in.)
.3150 (8 mm)
.3937 (10 mm)

** Amplified sinewave is limited to 500 cycles.

*For encoders to be mounted on PMI Motors, use the following table.

Motor	Hub
U9 Series	.4995
U9M4HA-2	.3745
U12 Series	.4995
S6 Series	.3150

All specifications subject to change without notice.

49 Mall Drive • Commack, NY 11725-5703 • (516) 864-1000 • Telex 510-223-0007

PMI MOTION TECHNOLOGIES
Division of Kollmorgen Corporation

© 1983 Printed in U.S.A.

5-86/MAR-089B

VITA

Richard David Turner was born in Knoxville, Tennessee, on September 10, 1966. He graduated from Halls High School, Knoxville, Tennessee, in June of 1984. He entered the University of Tennessee, Knoxville in September of 1984 and worked toward a Bachelor of Science degree in Mechanical Engineering. He received his B.S. in June of 1988.

He entered the Graduate School of the University of Tennessee in August of 1988 and will receive his Master of Science degree in Mechanical Engineering in August of 1991.

His interests include jogging, weight lifting, and karate.